Engineering Center
University of Wisconsin-Madison

HIGH-RESOLUTION INTERFEROMETER MODIFICATION OF THE GOES L/M SOUNDER: FEASIBILITY STUDY

A REPORT from the

Cooperative
Institute for
Meteorological
Satellite
Studies

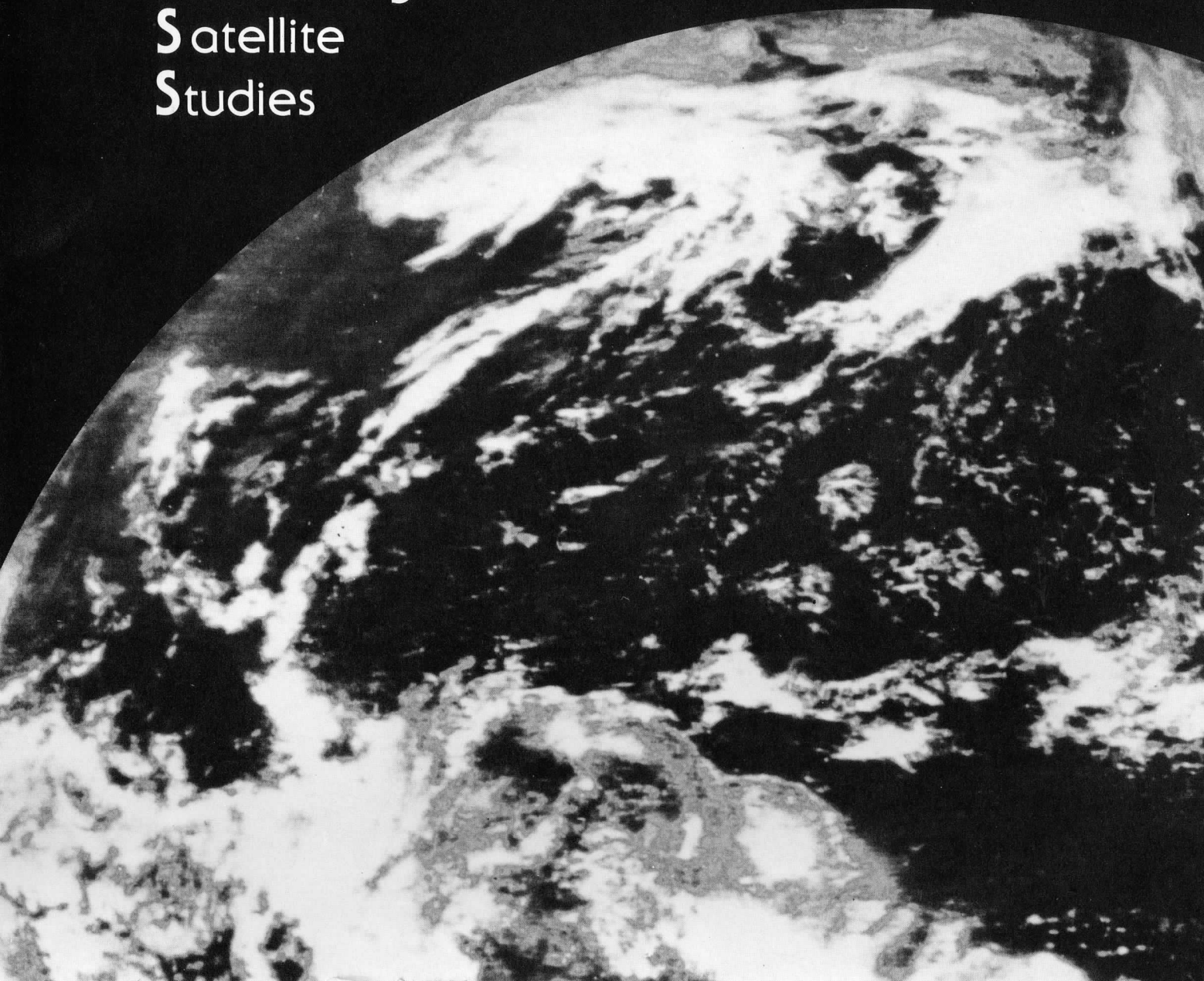

HIGH-RESOLUTION INTERFEROMETER MODIFICATION OF THE GOES L/M SOUNDER: FEASIBILITY STUDY

A Report To The:

National Oceanic and Atmospheric Administration (NOAA)
National Environmental Satellite, Data, and Information Service (NESDIS)
Washington, DC 20233

By:

University of Wisconsin-Madison
Cooperative Institute for Meteorological Satellite Studies (CIMSS)

Santa Barbara Research Center (SBRC)

ITT Aerospace/Optical Division

September 1988

RPT81280

RPT81280

CONTENTS

CONTENTS (CONT)

CONTENTS (CONT)

LIST OF ILLUSTRATIONS

LIST OF ILLUSTRATIONS (CONT)

TABLES

EXECUTIVE SUMMARY

This is the report of NOAA/NESDIS Grant number NA87AA-H-SP085 for the High-resolution Interferometer Modification of the GOES I/M Sounder: Feasibility Study. The study confirms that the replacement of the GOES sounder filter wheel with an interferometer is feasible and, further, that it is a very attractive way to obtain a major enhancement in vertical sounding resolution and accuracy.

STUDY ORGANIZATION

The study was a joint effort among ITT Aerospace/Optical Division, Santa Barbara Research Center (SBRC), and the University of Wisconsin-Madison (UW), with review and direction from NOAA/NESDIS. ITT, the GOES I/M instrument subcontractor, provided the current instrument constraints and interface definition, SBRC provided the conceptual design and feasibility assessment of the interferometer module, and UW provided sounding performance evaluation, program management, and experimental performance assessments using the High-resolution Interferometer Sounder (HIS) aircraft instrument. Prior experience of UW and SBRC with the HIS aircraft instrument and the 1981 NOAA/NASA conceptual design study for a geosynchronous interferometer sounder provided a strong foundation for the evolution of a mature interferometer design.

USE OF GOES I/M SUBSYSTEMS AND MAINTENANCE OF OPERATIONAL MODES

The modification requires no substantial changes to the major GOES I/M subsystems for earth pointing (scan mirror), calibration (reference blackbody), energy collection and image formation (telescope), and detector and instrument temperature control (two passive radiative coolers) and maintains many of the general characteristics of the GOES I/M. The existing earth scanning modes and footprint are maintained in the design, and only minor modifications are necessary in the mass and power envelopes, with no change in volume.[1]

INSTRUMENT MODIFICATION

The design modification involves replacing the filter-wheel assembly and relay optics with an interferometer assembly that would be temperature controlled using the same secondary radiative cooler currently used for the filter wheel. The desired performance of the complete instrument is achievable without substantial changes to the cold portion of the aft optics, except that detectors with higher responsivity would be used.

SOUNDING PERFORMANCE

Not only will the modified sounder provide greatly improved vertical resolution and accuracy from the high-resolution interferometer modes (as proven by the performance of the HIS aircraft instrument), but even the sounding performance of the most rapid global coverage (0.1 second stepping time) will be greatly enhanced. The primary improvement for the low-resolution, global mode will result from the large reduction in noise, especially in the 15 μm band where the interferometer multiplex advantage is highest. Improved spectral coverage, resolution, and band definition should also result in important improvements.

DATA RATES

The data-rate penalty for the substantial sounding improvement is modest. The highest rate for the design presented here is less than 500 kbps for on-board processing to spectra with no data compression. Data compression techniques to reduce this rate by factors of between 2 and 5 can be implemented, if necessary, and should be studied in more detail in the next phases of this program.

[1] An additional electronics module will be mounted on the spacecraft.

RELIABILITY

The modified instrument would be extremely reliable. Flex pivots are used to support the interferometer moving mirror and the dynamic alignment mirror to eliminate the wear associated with contacting surfaces. As a result, the reliability of the design will be as good as the reliability of the electrical drive systems, which can be designed to be redundant. The laser used for accurate optical-path sample control and Michelson-mirror dynamic alignment is very reliable because it uses diode-pumped YAG laser technology, which has matured in the last few years and is currently undergoing space-flight qualification. The laser will be made internally redundant through the use of multiple, pumped diodes. Redundancy is also designed into the on-board processor and other electronics. We expect the probability for a 10-year lifetime to be very high.

The instrument concept developed in this feasibility study would provide a very important new sounding capability for improved forecasting and would be an important complement to the improved forecasting models of the next decade. The study was based on the plan of implementing the change on the L and M models of GOES I/M. If this plan should not be feasible, other options for implementation at an early date should be investigated.

PART I

OVERVIEW AND FEASIBILITY SUMMARY

(UNIVERSITY OF WISCONSIN)

Section 1
OVERVIEW

Because of the temperature profiling capabilities needed to meet the 1990s initiative for improved mesoscale weather prediction, the remarkable performance history of Michelson interferometry, and the recent successful aircraft demonstration of the High-resolution Interferometer Sounder (HIS) technology, the time is right to proceed with plans to place interferometer sounders on geosynchronous satellites during the next decade. The objective of this report is to show, in detail, the engineering feasibility of this plan. A cost assessment for modifying the GOES I/M sounding instrument to measure high-resolution spectra with an interferometer is presented in a separate report.

Higher vertical resolution temperature soundings from geosynchronous orbit are needed to make full use of the improved wind observations planned for the 1990s. For mesoscale weather prediction, it is important to have observations of both temperature and wind distributions that together provide information on vertical motion fields. Improved wind measurements will soon be available to enhance our nation's weather prediction capability, since NOAA is installing a network of 30 Doppler radar wind profilers, spaced 500 km apart, across the midwestern U.S. During the 1990s, it is planned to expand this network eastward to the coast with the ultimate goal of replacing the rawinsonde. The Doppler radars provide wind profiles on an hourly basis with an accuracy of 1 m/s and a vertical resolution of 1 km. However, the profiler does not measure atmospheric temperature and water vapor.

To allow vertical motion fields to be determined from profiler winds and GOES-acquired temperature measurements, it can be shown (using the thermal wind relationship) that the temperature distribution must be observed with a vertical resolution of 1-2 km and an accuracy on the order of 1°C. The initial GOES I/M filter-wheel instrument will fall far short of meeting these goals, as will be demonstrated in the following subsection. Experience with GOES-VAS data confirms the fact that geostationary satellite temperature profile data with the poor spectral (vertical) resolution provided by filter-wheel radiometers offer little information on mesoscale phenomena. The primary uses of the VAS instrument for mesoscale applications have been in the definition of the water vapor structure from the sounding retrieval process and the diagnosis of the horizontal wind field by tracking cloud and water vapor motion.

In summary, greatly improved temperature profile resolution and accuracy from the GOES I/M instruments are needed to meet the mesoscale meteorological data requirements of the next decade and beyond.

PERFORMANCE IMPROVEMENT FROM THE INTERFEROMETER APPROACH

To attain the vertical temperature profile resolution required, the sounding instrument must achieve a spectral resolution of 0.1% ($\Delta\lambda/\lambda$) to avoid smearing the upwelling radiance contributions from relatively opaque absorption lines with the contributions from more transparent regions in between the opaque absorption lines. For example, in the thermal emission bands of CO_2, a spectral resolution of 0.7 cm^{-1} is needed in the 600-700 cm^{-1} (15 μm) region and 2 cm^{-1} in the 2300-2400 cm^{-1} (4.3 μm) region. Although this spectral resolution is beyond the capabilities of filter-wheel radiometers, it can be achieved using an interferometer.

The HIS aircraft instrument aboard the NASA U-2 and ER-2 aircraft has proven the performance capabilities of an interferometer. Ground calibration tests and airborne science missions have demonstrated the ability of the HIS to measure radiometrically accurate emission spectra with a resolution far exceeding the performance of contemporary radiometers. Radiance spectra have been obtained during more than 30 aircraft missions with a resolution of 0.35 cm^{-1} in the 600 to 1100 μm region, as compared to the typical 15.0 cm^{-1} resolution of filter radiometers, such as the one planned for GOES I/M.

Figure 1 shows a typical spectrum of infrared radiation brightness temperature sensed by the HIS. The half-bandwidths of the filters planned for the initial GOES I/M sounding radiometer are superimposed. As can be seen, the filter-wheel radiometer severely smears the fine scale spectral radiance structure of the atmosphere. This spectral smearing causes unwanted absorption contamination in atmospheric "windows" used for sensing the earth's surface temperature, and it greatly limits the vertical resolution of temperature and water vapor profiles because it broadens the atmospheric weighting functions.

Figure 2 shows more clearly the effect of spectral resolution on radiance smearing. It can be seen from these brightness temperature spectra that the 15 cm^{-1} resolution of the GOES I/M filter-wheel instrument causes an extreme smearing of energy emission from the lower atmospheric levels (brightness temperatures in excess of 240K) with energy emission from upper atmospheric levels (brightness temperatures below 240K) as revealed in the high-resolution brightness-temperature structure observed by the HIS.

Figure 3 compares the vertical resolution of atmospheric temperature profiles as sensed by the GOES I/M filter-wheel radiometer to those of the interferometer sounder. Figure 4 shows the expected sounding accuracy of the GOES I/M filter instrument compared to the proposed modified version. Simulations also demonstrating these substantial improvements in accuracy have been performed by Henry Fleming of NOAA/ NESDIS. As can be seen from Figures 3 and 4, dramatic improvements in vertical resolution and accuracy would result from the interferometer modification.

Possibly the most important application of the GOES interferometer will be the tracing of fine scale features of the atmosphere's water substance. The interferometer sounder is capable of sensing water vapor emission with very high vertical resolution. From the geostationary satellite, observations of the dynamic displacement of fine vertical scale water vapor features might be used to construct vertical wind-velocity profiles as well as to provide a direct measure of the moisture convergence responsible for weather development. The unique moisture structure sensing capability of the interferometer, together with its associated improved temperature profiling performance, are considered crucial for the use of geostationary satellite data in the mesoscale numerical weather-prediction models planned for the next decade and beyond.

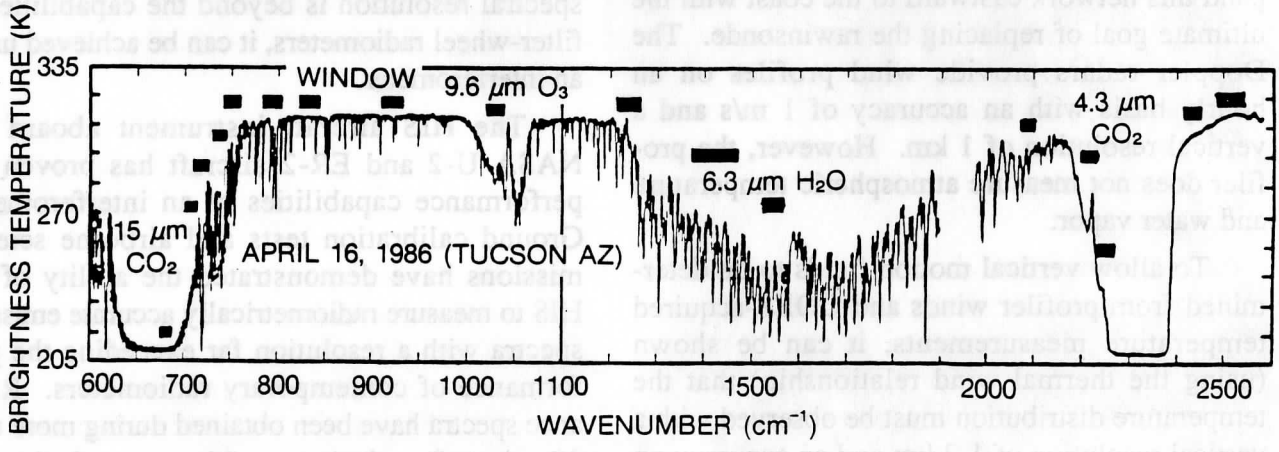

Figure 1. Radiation brightness temperature spectrum as observed by HIS from the NASA U-2 aircraft over Tucson, Arizona with the half bandwidths of the GOES-NEXT filters superimposed

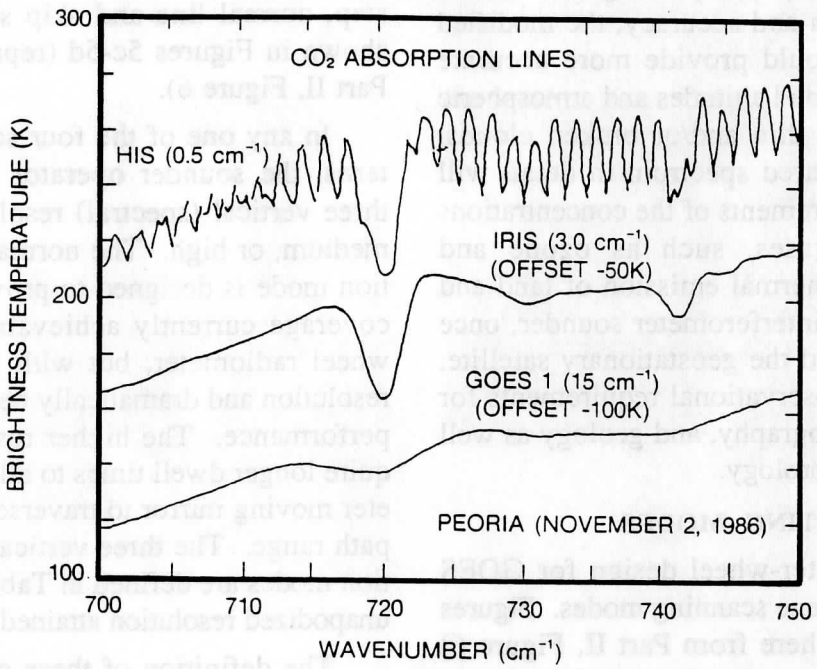

Figure 2. Brightness temperature spectra showing how emissions from different atmospheric levels are smeared by low-resolution measurements, which cannot resolve the CO_2 lines.

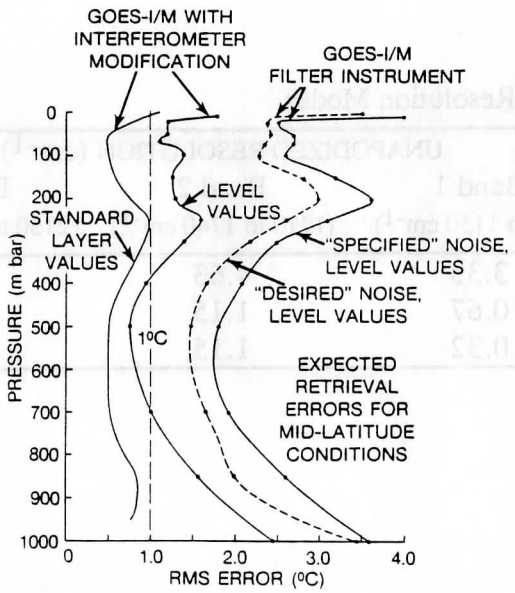

Figure 3. Improvement in vertical temperature profile resolution from modifying GOES L/M to use an interferometer.

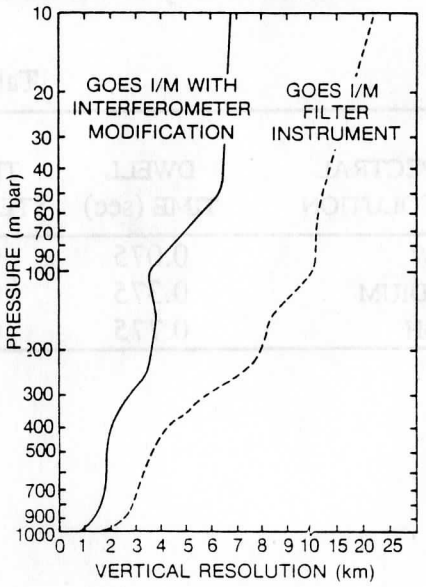

Figure 4. Improvement in vertical temperature profile RMS retrieval errors from modifying GOES L/M to use an interferometer. The "Standard Layer Values" curve denotes the result for the retrieved temperature, vertically averaged within the layers bounded by the levels, shown as dots on the other curves.

In addition to greatly improving atmospheric sounding resolution and accuracy, the modified GOES Sounder would provide more accurate measurements of cloud altitudes and atmospheric soundings beneath thin and/or broken clouds. Observing the infrared spectrum in detail will also provide measurements of the concentrations of atmospheric gases, such as ozone and methane, and the thermal emission of land and sea surfaces. The interferometer sounder, once implemented aboard the geostationary satellite, will help satisfy observational requirements for climatology, oceanography, and geology as well as operational meteorology.

SOUNDER OPERATING MODES

The current filter-wheel design for GOES I/M contains two scene scanning modes. Figures 5a-5b (reproduced here from Part II, Figure 6) show the scan patterns for the existing single-step, normal-line and single-step, skip-line modes. Two new scene scanning patterns have been introduced to fully utilize the capabilities of the interferometer. The new scan patterns (skip step, normal line and skip step, skip line) are shown in Figures 5c-5d (reproduced here from Part II, Figure 6).

In any one of the four scene scanning patterns, the sounder operator has the choice of three vertical (spectral) resolution modes; low, medium, or high. The normal step, low-resolution mode is designed to provide the same area coverage currently achievable with the filter-wheel radiometer, but with improved spectral resolution and dramatically better signal-to-noise performance. The higher resolution modes require longer dwell times to allow the interferometer moving mirror to traverse the longer optical path range. The three vertical (spectral) resolution modes are defined in Table 1 in terms of the unapodized resolution attained in each band.

The definition of these operating modes is based on a desire to maintain most of the operational characteristics of the GOES I/M sounder.

Table 1. Vertical Resolution Modes

SPECTRAL RESOLUTION	DWELL TIME (sec)	TIME / STEP (sec)	UNAPODIZED RESOLUTION (cm^{-1}) Band 1 (620 to 1150 cm^{-1})	Band 2 (1210 to 1740 cm^{-1})	Band 3 (2150 to 2721 cm^{-1})
LOW	0.075	0.1	3.33	4.63	4.63
MEDIUM	0.375	0.4	0.67	1.15	1.15
HIGH	0.775	0.8	0.32	1.15	1.15

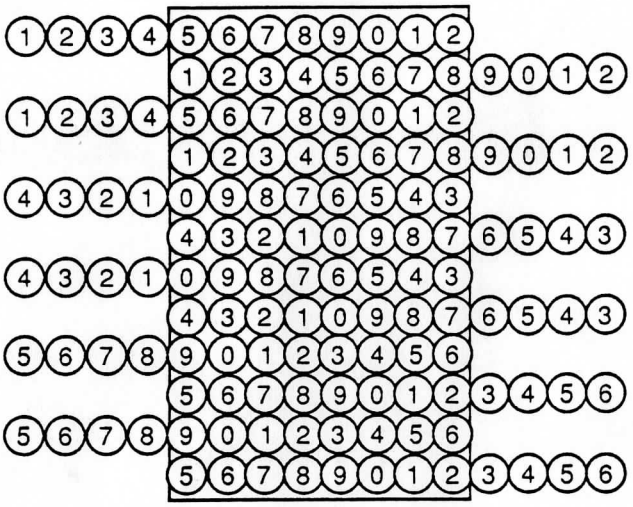

Figure 5a. Single step, normal line

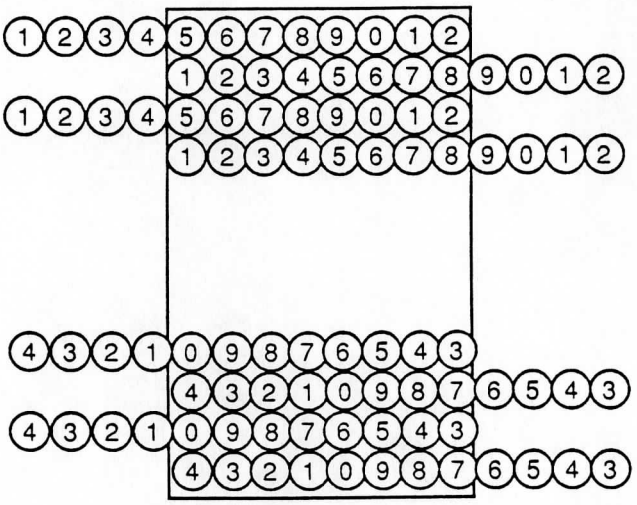

Figure 5b. Single step, skip line

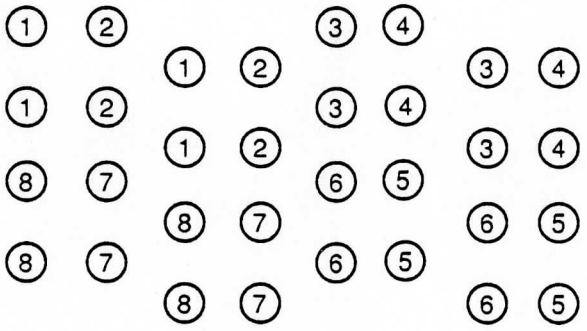

Figure 5c. Skip step, normal line

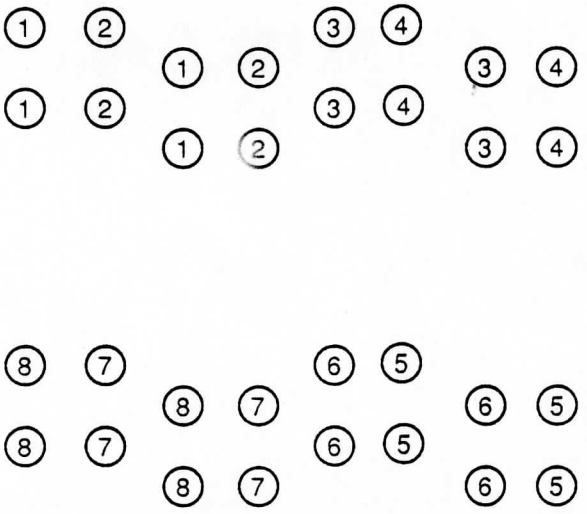

Figure 5d. Skip step, skip line

Figure 5. Sounding in different scan modes (Dwell 0.1, 0.2, 0.4, 0.8s at each location)

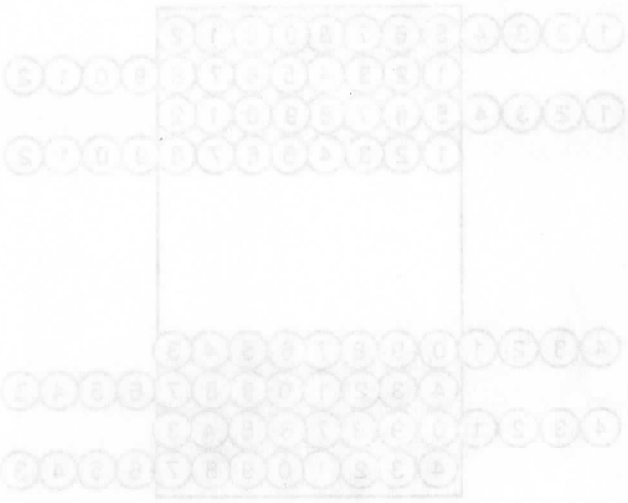

Section 2

FEASIBILITY CONSIDERATIONS

The results of the feasibility study to modify the GOES filter-wheel sounder to incorporate a high-resolution interferometer are summarized in this section.

INTERFACE TO EXISTING SYSTEM

The modularity of the GOES Sounder makes implementation of the interferometer modification quite feasible. The existing scene-mirror optics and its control circuitry will remain unchanged. Some reprogramming of the scene mirror will be required to accommodate the new scan modes; however, the digital GOES design is well suited to accepting such changes. The existing passive cooler, used to cool the aft optics, detectors, and focal plane will be maintained. Also the physical dimensions of the sensor assembly will remain unchanged. The filter-wheel passive cooler will be used to cool the interferometer module. The major change is to remove the filter wheel and relay optics from the input beam and to replace them with an interferometer and its relay optics. Another change is to replace the electronics circuitry with circuitry appropriate for controlling the dynamically aligned interferometer and for on-board processing of the data. The last change is to replace the current set of detectors with ones optimized for the interferometer's long-wavelength (LW), mid-wavelength (MW), and short-wavelength (SW) bandpasses.

MASS

The mass of the interferometer and the mass of the electronic control circuitry being added (10 lbs) nearly equals the mass of analogous material being removed (11 lbs). The main additional mass (16 lbs) being added in the interferometer design is for the on-board processing system, which has no analog in the filter-wheel sounder.

The total system mass is expected to be only about 5% greater than the mass of the current filter wheel sounder.

POWER

The modification requires an additional 10.7W of average power, including 5.2W for the data processing on board. The interferometer adds no additional peak power requirements, and the additional average power is within the current margin for power available to the sounder.

VOLUME

Using careful optical design, the entire interferometer assembly and relay optics fit easily into the volume housing the current filter wheel and associated optics. A three-dimensional drawing showing the interferometer optical elements as they will fit into the available volume is given in Figure 6.

DETECTOR PERFORMANCE/COOLING REQUIREMENTS

The detectors in the ITT design will be replaced by detectors optimized for the interferometer LW, MW, and SW bands. Table 2 summarizes the expected noise performance for a 2 cm^{-1} resolution spectrum, as specified for the Interferometer Modification of GOES I/M (Sect. 4), assuming a 4 cm/sec moving mirror velocity. This is discussed in greater detail in Part III.

Note that the NENs for soundings will be better than those shown in Table 2 by a factor of the square root of the number of clear FOVs per sounding.

The existing passive cooler is adequate to achieve the desired level of performance with the addition of new temperature set points to account for seasonal temperature variations.

DATA RATE

The expected data rate is based on the use of Digital Signal Processor (DSP) modules to do on-board Fourier transforms of the interferogram data in real time. Table 3 gives the data rates for the full spectra (all bands included). For each item in the table, the higher number holds if complex spectra are computed, the lower number if magnitude spectra are used. In all cases, the data rates are less than 500 kbps.

Further reductions in data rate (by a factor of 2 to 5) could be realized with data compression.

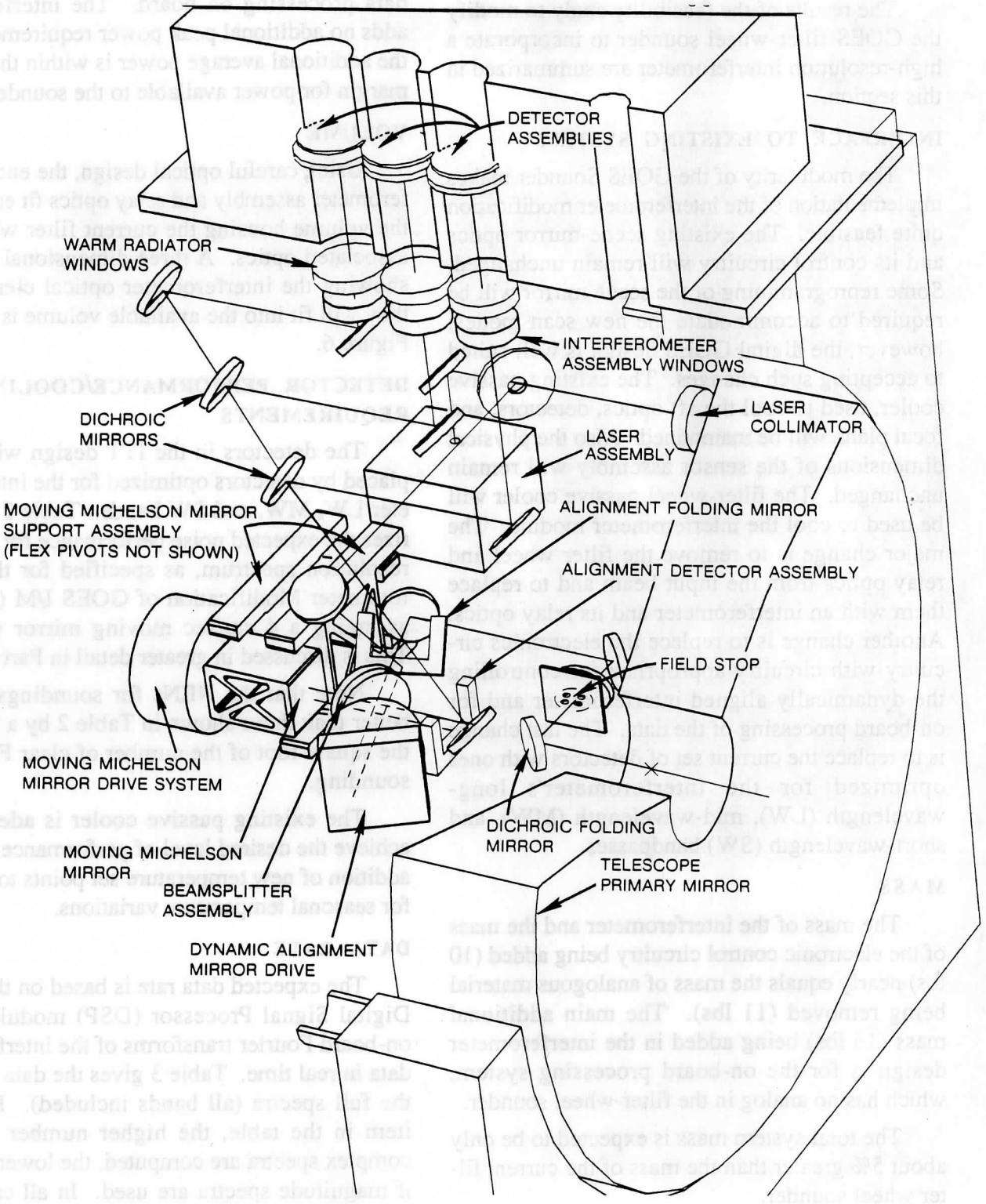

Figure 6. Interferometer optomechanical module

Table 2. The Required and Expected NEN Performance at 2 cm^{-1} Unapodized Spectral Resolution and 0.125 sec Integration Time

BAND	NEN REQUIREMENT (mW/m^2 sr cm^{-1}) SPECIFIED	DESIRED	EXPECTED
1	0.44	0.2	0.145
2	0.12	0.04	0.076
3	0.01	0.0035	0.0084

Table 3. Data Rates For The Interferometer Sounder By Operating Mode

SPECTRAL RESOLUTION	TOTAL DATA RATE (kbps) SINGLE STEP, NORMAL LINE/ SKIP STEP, SKIP LINE	SKIP STEP, NORMAL LINE/ SKIP STEP, SKIP LINE
LOW	452 / 226	226 / 113
MEDIUM	452 / 226	362 / 181
HIGH	336 / 168	299 / 149

DATA PROCESSING

The electronics conceptual design is based on the design of the Thermal Emission Spectrometer (TES), under development at SBRC. The fundamental processing unit of that design is a DSP module containing data RAM and a Texas Instruments TMS320C25 microprocessor. The function of this unit is to perform an FFT on a digitized interferogram and output the individual spectral channels obtained. UW-SSEC, has built an enhanced version of the DSP module using low-power CMOS technology and optimized FFT algorithms. The results of breadboard tests show that a complete FFT of the high-resolution data can be accomplished in less than 100 ms while dissipating less than 1.75W per DSP module. These processing times ensure that all four detectors could easily be processed in series within the times available in the current design.

VARIABLE VELOCITY OPD SCAN

As a part of this feasibility study, the University of Wisconsin performed a series of tests with the HIS aircraft instrument to determine the feasibility of using a variable speed OPD scan mirror to optimally scan selected regions of the Band 1 interferogram with higher signal to noise. The variable speed drive would provide a more uniformly distributed signal-to-noise ratio in the interferogram, thereby reducing the dwell time needed to obtain a specified temperature retrieval performance. The results of these tests are documented in the appendix to this report.

Although variable velocity OPD scanning was not needed to meet the performance requirements of the proposed GOES modification, it was shown to be a feasible approach. Having demonstrated the feasibility of variable velocity OPD scanning, the detailed tradeoffs between its performance improvement and complexity should be considered in Phase B.

Section 3

RELIABILITY AND RISK ASSESSMENT

RELIABILITY

The following items will not be modified, so their reliability should be determined from the GOES I/M sounder reliability studies:

- Scene Mirror and Bearing
- Fore Optics Telescope and Baffles
- On-board Blackbody Calibration Source
- Visible and Star Sensors
- Radiative Cooler and Cooler Cover
- Spacecraft Data and Power Interfaces.

The reliability of the following items, specific to the interferometer design, are discussed in detail in Part III and summarized below:

- Optical Elements
- Flex Pivots for Michelson mirror
- Detectors
- Laser and Drivers
- Electronics

The optical elements will maintain their high quality indefinitely, since experience shows that contamination can be prevented. Flex pivots designed within their operating capability have no points of wear and thus can have extended (10 years and greater) lifetimes. The windings of the drive motors can be made redundant to achieve a very high degree of reliability. The laser system is made reliable by the use of a solid rod of YAG laser gain medium with multiple diode drivers for redundancy. When operated at their design temperature, the expected lifetime for the diodes can easily meet the lifetime requirements. Statistics show that the reliability of the space sensor's electronics is the most critical element in determining overall instrument reliability. As a result, all of the electronics in the proposed modified design have redundant counterparts.

The GOES processing design has three parallel processing threads, one for each of the LW, MW and SW bands. The computational engine for each thread is a Digital Signal Processor (DSP) module, which does an FFT on the digital interferograms. SBRC has recently completed an analysis showing the DSP modules to be used in the GOES design have a probability of 0.9934 of successfully completing a 5-year period of continuous operation, and these modules are redundant in the proposed design.

In summary, the current design is highly reliable and demonstrates the feasibility of the sounder modification. In addition, the design can be readily modified to increase the fail-soft nature of the system.

RISK ASSESSMENT

Table 4 summarizes current estimates of performance risk, and risk to schedule, cost, and weight.

Table 4. Performance Risk Assessment

Risk Summary	**•Normal to Moderate Risk To Schedule, Cost, Power, and Weight •System Compatible With Today's Technology •Normal Risk to Achievement of Science Goals**	
Performance Requirement	**Performance Risk***	**Remarks**
Stepping & Coverage	Normal	• Pointing Stability During An Interferometer Scan May Be The Driving System Stability Requirement
Spatial Resolution	Normal	• Small IFOV Will Cause Diffraction or Blur Challenges
Spectral Intervals	Moderate	• Continuous and Contiguous Wavelength Requires 3 Detector Bands **No New Detector Technology Required**
Spectral Resolution	Normal	• Very Well Controlled, Mathematically Derived Channel Shape Inherent In FTS Concept • All Detectors In Detector Array Have Mathematically Derivable Spectral Response Functions • **No In-flight Measurement Needed** • Can Change Spectral Shape With Ground Processing If Desired • Sidelobe Response < 0.5%
Signal Noise	Moderate	• Bands 2,3 Require Moderate Cooling of Optical System (Single Stage Filter-Wheel Radiative Cooler)
Radiometric Calibration	Normal	• Blackbody and Space Look Each Scan • **Techniques Fully Demonstrated** • **Not Interferometer Specific**
Stray Sources of Radiation	Normal	• Good Optical Design Practices Insure Low Out-of-FOV Source Sensitivity • Some Internal Diffraction Problems • FTS Approach Limits Sensitivity To Stray Radiation
Programmable Output	Low	• Continuous and Contiguous Wavelengths Are Transmitted

Table 4. Performance Risk Assessment (Cont)

Technology Area	Schedule, Cost, Power, Weight Risks*	Remarks
Interferometer	Normal	• **No Real Optical Design Challenge**
Optical Design		• Concepts Well Proven In ER2 "HIS" Instrument
Optical Materials	Normal	• Beamsplitter Needs Special Mounting Care
Optical Elements	Normal	• Small Size of Detector Field Lenses Will Require Extra Effort
Reference Laser	Moderate	• Laser Rod is From Flash Lamp Pumped Laser Technology Well Developed, Reliable, Rad Hard, and Available • Pumping Diodes are From Communications Technology Reliable, Low Power, Rad Hard, Redundant, and Efficient • Space Qualified Laser Diodes Available Now • CW Diode Pumped 1.06μ Lasers are Now Commercially Available • Many Diodes Can Be Used To Pump The Laser Providing Redundancy for Long Life • Screening Requirements Need to Be Developed • **No New Technology Needed**
Dynamic Alignment	Moderate	• Concepts Well Demonstrated In ER2 Instrument • New Implementation • **No New Technology Needed**
Michelson Mirror Drive	Moderate	• Concepts Demonstrated In SBRC IR&D Programs, XM21 Program and AFGRLs Aircraft and Flight Programs • Thematic Mapper Scan Mirror Flex Pivot and Drive Technology
Preamplifiers and Filters	Low	• Good Engineering Practices Insure Low Noise and Linear Phase
S/H & A/D Converters	Normal	• Current Parts Need Screening
Digital Signal Processor	Moderate	• Packaging Issues - No Performance Issues
Command, Telemetry	Low	• Good Engineering Practices Ensure Efficient &Reliable System Formatting & Control
Power System	Normal	• Good Engineering Practices Ensure Efficient &Reliable System
Detectors	Moderate	• While **No New Technology Is Required** Detectors Always Take Special Attention • Reasonable Size Detectors

***Low risk**	Straightforward engineering.
Normal risk	Typical encountered in NASA Phase B/C flight programs
Moderate risk	Special attention required but with limited development costs.
High risk	Technology breakthrough required.

Section 4

SPECIFICATION FOR THE INTERFEROMETER MODIFICATION OF THE GOES I/M SOUNDER

The specification to which the interferometer modification was designed is presented in this section.

The current GOES I/M Sounder is being built by ITT according to Ford Aerospace and Communications Corporation Specification No. 565054, DOC CODE SE, entitled "Sounding Subsystem Performance Specifications." Whenever relevant, and whenever technically possible, the modified sounder will be designed to the same specifications. Modifications to Section 3.2 of the Ford specification, Performance Characteristics, required by the difference in the performance of a filter-wheel radiometer and an interferometer are stated below:

The major section requiring change is Paragraph 3.2.1 Sounding Channel Requirements. The changes are as follows:

3.2.1.1 Spectral Requirements. The spectral bandpass of the interferometer module shall be divided into three bands, long wavelength (LW), mid wavelength (MW), and short wavelength (SW) as in the current instrument, with each band using a separate 2 × 2 detector array. All of the current filter-wheel channels for a given band will be sensed by the same band of the interferometer module. The minimum spectral coverage of each band is defined as: Band 1, 673 to 1048 cm^{-1}; Band 2, 1322 to 1565 cm^{-1}, Band 3, 2176 to 2721 cm^{-1}.

The spectral resolution of the interferometer data shall be selectable. The resolution in each band in the lowest resolution, rapid-coverage mode will exceed the resolution of all channels in the filter-wheel design in the same band (see p. III-10). The interferometer will be capable of achieving resolutions (unapodized) of 0.33 cm^{-1} (1.5 cm maximum delay) in the LW band, and 2.0 cm^{-1} (0.25 cm maximum delay) in the MW and SW bands.

3.2.1.2 Sensitivity Requirements. This specification will not change for the lowest spectral resolution, rapid-coverage mode (0.1 second dwell). The noise in the current channels will be determined from the interferometer data by averaging over the nominal bandpass of the current filter-wheel specifications.

The NEN specification for the higher-resolution modes will be based on the performance for resolutions of 2.0 cm^{-1} in each band (0.25 cm maximum delay). The spectral noise equivalent radiances of Table 3-3 of the Ford instrument specification shall apply to 2.0 cm^{-1} resolution spectra with a dwell time of 0.4 seconds or less. During the same dwell time, the delay region from 0.50 to 0.75 cm shall be sampled in the LW band with a noise level in the interferogram that is at least two times smaller than that corresponding to the specifications for the delay region out to 0.25 cm.

3.2.1.3 Out-of-Band Spectral Response and 3.2.1.4 Out-of-Band Spectral Response Verification These requirements are not needed for the interferometer approach.

Other changes to the Ford instrument specification are as follows:

3.3.2.4 Selected Dwell Time. Filter-wheel rotations should be interpreted as periods of 0.1 seconds.

3.2.4.1 Scanning Requirements. Two scan modes, which allow more versatile coverage, will be added. One steps repeatedly 2 × 280 μr, 6 × 280 μr, 2 × 280 μs, 6 × 280 μs, etc. This permits sampling every other of the current IFOVs. The other has the same stepping pattern and, in addition, skips every other horizontal scan line.

PART II

GOES I/M INTERFACES AND MODIFICATIONS

(ITT AEROSPACE/OPTICAL DIVISION)

Section 1

INTRODUCTION

The GOES Sounder is presently in assembly for use on the GOES I-M series of operational spacecraft. This instrument has a design heritage from the TIROS/NOAA High Resolution Infrared Radiometric Sounder (HIRS) which is based on discrete filters for spectral channel definition. In order to advance the quality of soundings the GOES Sounder will be modified to replace the filter assembly with an interferometer assembly.

Modular design of the GOES Sounder provides the opportunity to make this change with a minimum effect on design, fabrication or operation. This part of the report will discuss the functional operation of the Sounder and the implications of the proposed changes.

Section 2

KEY FEATURES

The primary operating characteristics of the GOES Sounder will be retained. The only functional change will be to expand the flexibility of the scan system to permit an optional longer dwell time at each sounding location, and another optional skip-step mode to permit faster soundings over large areas.

As a consequence of the richer data set collected by the interferometer the output data rate will increase from 40,000 bits per second to as much as 500,000 bits per second. Other changes, internal to the system, will be made such as to correlate the earth scanning mirror motion with the interferometer delay mirror scan.

Key features of the GOES High Resolution Interferometer Sounder (GHIS) are given in Table 1. Items modified or added for the new system are highlighted. It may be noted that these changes are a small part of the system, indicating the compatible nature of the interferometer.

Table 1. Key Features of Sounder

Simultaneous FOV	4
FOV Defining Element	Field Stop, 242 μrad (8.6 km, Nadir)
Telescope Aperture	31.1 cm (12.25 in) Diameter
Channel Separation, LW-SW-MW	Dichroic
IR Spectral Definition	Interferometer*
Visible Sounding	Fixed Detectors
Radiometric Calibration	Space and 290K-IR Blackbody
Frequency of Space Clamp	2 Minutes
Frequency of IR Calibration	20 Minutes
IR Detector Operating Temperature (K)	92*, 97*, 102, 107
Field Sampling	4 Areas N-S on 10 km Centers
Scan Step Angle	280 μrad (10 km Nadir); Skip-Step* and Skip-Line Optional
Step and Dwell Time	0.1 Seconds; 02.s, 0.4s, 0.8s* Optional
Scan Capability	Full Earth and Space
Sounding Areas	10 km × 40 km to 60° N-S and 60° E-W
Optical Location	Star Sensing
Output Data Quantizing	12 Bits all Channels*
Output Data Rate	<500 kbits Per Second Without Data Compression (lower by 2 to 5 times with compression)*
System Power Average	112W
System Weight:	
Sensor Assembly	202 lb (92.0 kg)
Electronics Module	61 lb (27.9 kg)
Power Supply	14 lb (6.2 kg)
Interferometer Processor*	16 lb (7.3 kg)
Total	293 lb (133.4 kg)

* Added for interferometer.

Section 3

INSTRUMENT DESCRIPTION

The GOES Interferometer Sounder is intended to provide improved data for atmospheric temperature and moisture profiles, surface and cloud top temperature and ozone distribution. The GOES I Series Sounder, as a separate instrument, provides a higher area coverage rate than any previous Sounder and has sufficient sensitivity for operational soundings from every sample. The inclusion of the interferometer extends the capability to ever more precise profiles without sacrificing the operational features of the GOES Sounder.

The Sounder is composed of four basic modules, a Sensor Assembly mounted to the exterior of the spacecraft and an Electronics Module and Power Supply module mounted on an instrumentation panel internal to the spacecraft. A separate data processing module will be added for the interferometer data processing.

The Sensor Assembly, externally mounted to the spacecraft, contains the scan and detection components. The rectangular housing has an optical port to earth that is protected by a 23 cm sun shade. The shade reduces solar input to a relatively short period of the orbit. The telescope is an open truss design to reduce solar influence. When the sun does shine into the scan cavity, its energy is collected in a part of the housing structure that is not a part of the telescope and, therefore, reduces thermal effects that might cause a change in focus. Those parts of the instrument that receive solar input, whether direct or reflected from the scan mirror, are protected by baffles or absorb the energy with minimal effect on optical or radiometric response.

The primary mirror is mounted in a stable bulkhead, which is the optical reference and also holds the truss network. The mirror is mounted using tangent bars that permit slight motion during launch but retain alignment during operation.

SIGNAL FLOW

A 31.1 cm aperture telescope receives energy from the earth's surface/atmosphere, space, or the calibration blackbody as determined by the mirror scan angle. Detection of the infrared spectral features takes place in the interferometer assembly. As shown in Figure 1, the interferometer assembly operates on the single beam to detect the signal at each delay location. After optical processing the beam is split to longwave, midwave and shortwave bands very similar to the filter wheel sounder.

Although not viewed through the interferometer, the visible detectors are gated so that they sample the same atmospheric column at the same time as the IR channels.

The interferometer acts as the spectral defining element in the system. It also has a major effect on the radiometric stability and signal quality. From the interferometer to the detectors, there is no spectral limit other than a broadband limiting filter in the cooler. Any small deviation of radiance in this area may cause unwanted noise in the signal.

Cooling the interferometer to approximately 220K (compared to HIRS/2 operating at 296K) has three primary values: (1) to reduce emitted energy that might cause random noise; (2) to provide a very low background radiance input to the detectors to help improve detector detectivity; and (3) to reduce thermal loads on the cooler, permitting detector operation at 102K with adequate margin. The housing is thermally connected to a small radiative plate that has a view to the north and is isolated from solar input. With such a design, the interferometer operates at 220K with short-term (minutes) variations less than 0.05K and long-term (hours) variations less than 0.2K as established by a feedback-controlled heating system. This ensures both short-term and long-term radiometric stability.

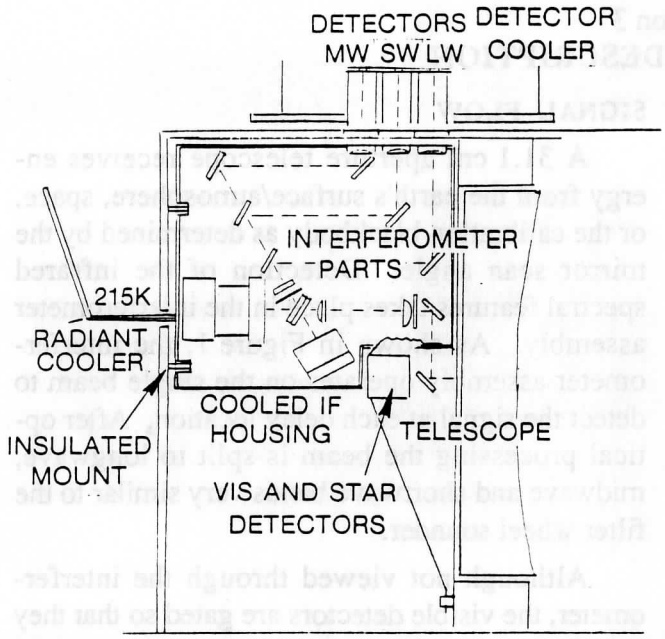

Figure 1. Interferometer assembly layout

Cooled Detectors

An array of four detectors in each band is arranged along the north-south (N-S) (longitudinal) axis. This array, as shown in Figure 2, generates an 1120 μrad N-S swath that is moved latitudinally in 280 μrad steps. The length of the scan is set by designated frame start and end coordinates.

Sets of four LW, four MW, and four SW detectors are mounted on the patch (third stage) of the radiative cooling assembly. It has capacity to offset the thermal input from the solar sail and boom. An addition to the cooler assembly is a loose fitting cover over the first stage shield that is opened after solar sail deployment and cooler outgassing. The cover, primarily required during transfer orbit when large solar inputs are likely, provides a means of protecting the cooler surfaces during prelaunch, launch, and orbit insertion when contamination control is difficult. The initial outgas period, when heat is applied to the cooler parts, requires less power with the cover closed. The cover is released by an Electro-Explosive Device (ESD) after solar sail deployment. A torsion spring swings the cover over the earth face of the instrument. Magnetic proximity switches monitor the closed and open condition of the cover.

Mechanical Assembly

The housing for the Sensor Assembly is designed for mechanical stability, ruggedness and thermal conduction. Stability is provided by a 7.6 cm thick machined aluminum base having a surface plate of 5 mm. This is heavier than required for strength alone and provides the stiffness that maintains alignment of the scan assembly, telescope, and cooler assembly. Machined panels complete the box structure. The heavy plate on the base, in combination with special shield, provides a thermal sink that distributes solar and control heat evenly throughout the instrument. This baseplate mounts to the spacecraft at six points having low thermal conductance, permitting the Sounder to be thermally independent of the spacecraft.

Electronic elements in the Sounder Assembly include preamplifiers for the 16 sounding detectors, for 8 star sensing detectors, and for the Inductosyn, where low level signals are amplified to levels suitable for cable coupling to the Data Processing Module. Other circuitry in the Sensor Assembly includes the power drive transistors for interferometer delay drive and the power drive transistors for the housing thermal control.

The Sounder scan components are duplicates of the Imager parts. An infinite-resolution torque motor drive and a high-resolution Inductosyn position sensor permits the scan to be controlled by the digitally derived signals applied to the Inductosyn. The drive motor moves the mirror to a null location, where it holds for the sampling time of the interferometer.

Thermal Control

Thermal control of the Sounder is key to maintaining radiometric stability and accuracy and reducing the number of radiometric calibrations. Diurnal variations of solar heating are offset by approximately 0.4 m^2 of louver-controlled cooling surface on the north panel. The louvers

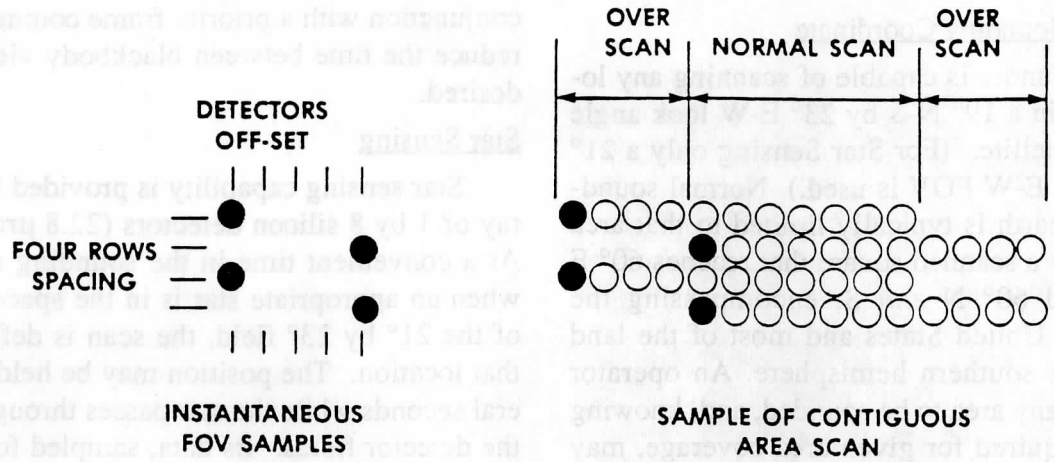

Figure 2. Detector separation and scan pattern

are closed at 13°C, begin to open at temperatures above that, and are fully open at 23°C, thus exposing the radiating area to space and cooling the housing. This occurs for about 3 hours each day as the sun shines into the scan cavity. Each individual louver element is independently controlled by its own bimetallic sensor, so that failure of any one has a minimal impact on system performance.

At other times, while the instrument is being cooled by the scan cavity looking at earth and space, electrical power is applied to the housing, maintaining a temperature no lower than 13°C.

Star Sensing

A star sensing array, consisting of a separate set of eight detectors, is on the same mount and aligned with the visible sounding detectors. It is identical to the Imager visible detector array but has a resolution of 0.82 km and an array coverage of 6.9 km. Each detector has a preamp and signal processing chain. Their data is collected 4 times each 0.1s and included in the Sounder output.

Electronics Module

The Electronics Module contains a card nest of approximately 100 multilayer printed circuit boards. A separate module contains the instrument power supply, and another module contains the data processing electronics for the interferometer.

Interfaces with the spacecraft are through several separate connectors and cables. Power and commands are received from the spacecraft, signal data, telemetry, and all housekeeping are sent to the spacecraft. The Sounder output data is totally independent of the Imager data, and is provided from redundant outputs. Signals are provided to the AOCS microprocessor for scan position compensation and analog signals are received that bias each scan.

All information required to generate a sounding is included in each data block which is developed each 0.1s. Each data block (sounding of four adjacent locations) has scan coordinates, radiometric and housekeeping information. Spacecraft attitude information is included to provide a total data base in each data block.

SOUNDER OPERATION

Flexibility of sounding operation in time and area coverage provides for rapid sampling of selected locations. This capability is provided by the fully digital controlled scan system using the discrete stepping capability of the Sounder. Simultaneous sampling of four locations and achieving operational sensitivity in all channels in only 0.1s time periods permits the collection of data in the time periods requested by the primary users of sounding data.

Selectable Sounding Coordinate

The Sounder is capable of scanning any location within a 19° N-S by 23° E-W look angle from the satellite. (For Star Sensing only a 21° N-S by 23° E-W FOV is used.) Normal sounding of the earth is typically limited to that area enclosed by a scanned square that reaches 60° E and W and 60° N and S, encompassing the continental United States and most of the land mass of the southern hemisphere. An operator may select any area to be sounded, and, knowing the time required for given area coverage, may program a series of scans that meets the operational or immediate needs. Requests are made in instrument scan coordinates for the beginning and end of each different area and for up to 15 identical repeats of any specific area. Scanning may move from north to south or vice versa, as desired. In a typical frame, the stepping begins at the operator selected location, steps from west to east to the end longitude location, moves south four fields and continues in a westerly step until all the area within the selected boundaries has been sampled. A typical pattern set to sound the conterminous states and adjacent ocean can be completed in 35 minutes.

Sounding Step/Time Flexibility

The basic 0.1s dwell time may be extended to 0.2, 0.4 and 0.8s for added delay range of the interferometer. The extended dwells permit finer and finer resolution of the atmospheric profile. In addition several discontinuous step patterns will be provided to permit rapid large area sounding coverage.

Radiometric References

While scanning within the earth scene, the instrument establishes radiometric references. Every 2 minutes, the scan control sends the mirror to look at space for a base value that measures the cold IR and black visible reference. As the spacecraft changes temperature in its orbit, the radiometric calibration is reestablished by a scan to a full-aperture blackbody, nominally each 20 minutes. A Calibrate Enable command in conjunction with a priority frame command may reduce the time between blackbody views if so desired.

Star Sensing

Star sensing capability is provided by an array of 1 by 8 silicon detectors (22.8 μrad each). At a convenient time in the sounding scenario, when an appropriate star is in the space portion of the 21° by 23° field, the scan is deflected to that location. The position may be held for several seconds while the star passes through one of the detector fields. Its data, sampled four times during each sounding period, provides signals for ground data processing that can define the star location permitting verification or adjustment of scan correction factors.

The command utilized to initiate the star sensing mode also inhibits normal IR calibrations, sets the dwell time at the commanded location and stores the current sounding location to enable return after star sensing.

Eclipse operation in a standby mode (to conserve power) is accommodated by maintaining interferometer temperature control during that period. This permits reduction of total power while maintaining the reference temperature, and with space and IR blackbody looks soon after eclipse, allows the Sounder to resume normal operation within a short time after full turn-on.

Output Data

Output data form the Sounder is estimated to be at a data rate of 500 kbps, which includes all radiometric, location, and telemetry data to make each sounding sample independent of all others. The data from the interferometer will be numerically filtered in a separate electronics module. The information is digitized and temporarily stored. The Sounder data system will clock the data into a selected portion of the data format.

Cooler Operation for Optimum Performance

The optimum sensitivity of the longwave detectors is achieved at the coldest temperature possible consistent with stable operation. The

design of the GHIS cooler will remain that of the GOES Sounder cooler. This implies that, if the detector bias power and optical port thermal inputs remain the same we can predict the annual variation of detector temperature. From the analyses performed for the GOES Sounder we can predict performance as shown in Figure 3. This indicates that for approximately 240 days of the year the detectors may be operated at 92K with as much as 5K of margin. For the remainder of the year the detectors may be operated at 97K with a slight change that during some orbits the patch may reach its thermal limit. If that happens the control may be reset for 102K. Changing from a cold to warmer set point may be accomplished in less than an hour requiring a nonoperational period. A change to a colder set point may require a day to stabilize, slow enough to permit accurate calibrations each 20 minutes.

A backup temperature set point at 107K is provided for potential failure mode control, but is not normally expected to be used.

The patch temperature control is set by relay selected resistor values in the proportionally controlled thermal control circuit. The change, then, is to add control relays for the new temperatures.

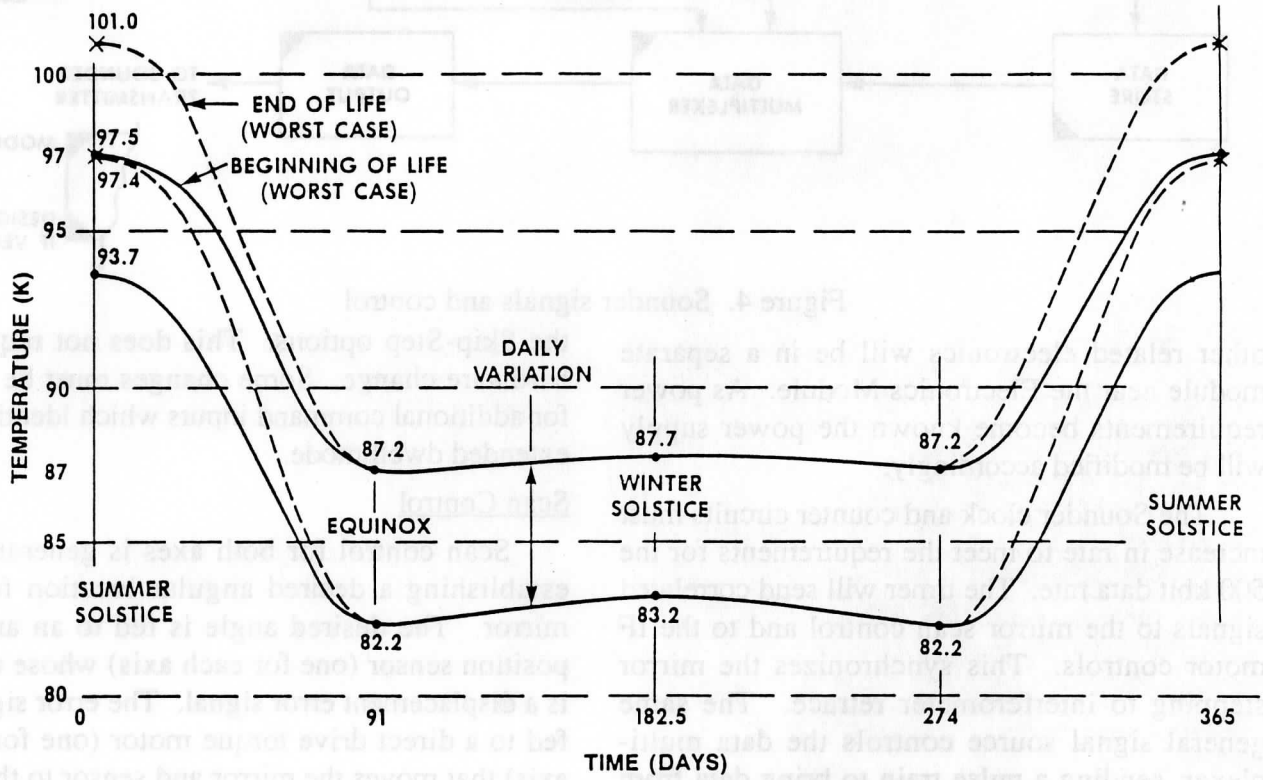

Figure 3. IR detector temperatures over annual cycle (uncontrolled patch)

SOUNDER ELECTRONICS

The signals and control electronics are shown in Figure 4. The circuits and parts represented by the corner markings will be designed by the Interferometer vendor. The IR detectors and optics which are a part of the detector/cooler assembly will be procured by ITT using the design requirements provided by the vendor. These parts will be defined in physical and electrical terms to permit the modifications necessary for integration. A GOES parts list has been given to the vendor for aid in component selections which will be most acceptable to the customer. Space will be made available in the Sensor Assembly for the preamplifiers, motor control and laser control The Interferometer control, numerical processor, data storage and

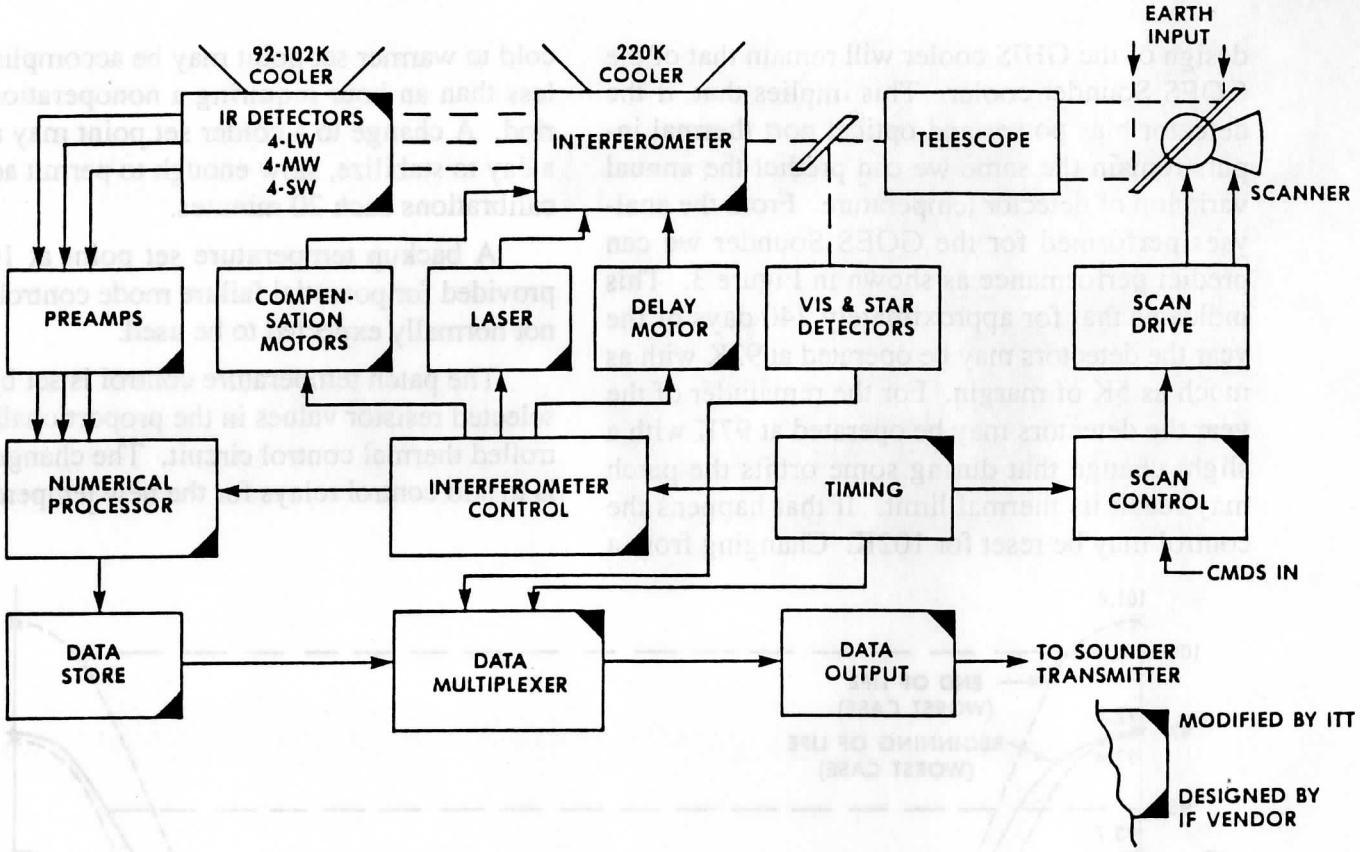

Figure 4. Sounder signals and control

other related electronics will be in a separate module near the Electronics Module. As power requirements become known the power supply will be modified accordingly.

The Sounder clock and counter circuits must increase in rate to meet the requirements for the 500 kbit data rate. The timer will send correlated signals to the mirror scan control and to the IF motor controls. This synchronizes the mirror stepping to interferometer retrace. The same general signal source controls the data multiplexer, sending a pulse train to bring data from storage into the multiplexed data stream. The amount of data to be stored will be in the order of 30K, which will be released only when a clock signal is received. These will be timed to file the data stream in accordance with a developed format. The MUX output drive system will be designed accordingly.

Scan control has several minor modifications. The programmable ROM can be reprogrammed to set the step dwell and step size for the Skip-Step options. This does not require a hardware change. Some changes must be made for additional command inputs which identify the extended dwell mode.

Scan Control

Scan control for both axes is generated by establishing a desired angular location for the mirror. The desired angle is fed to an angular position sensor (one for each axis) whose output is a displacement error signal. The error signal is fed to a direct drive torque motor (one for each axis) that moves the mirror and sensor to the null location.

For latitudinal deflection, the direct-drive torque motor is mounted to one side of the mirror and the position-sensing device (inductosyn magnetic position encoder) is mounted to the opposite side. All rotating parts are on a single shaft, with a common set of bearings. Coupling of the drive, motion, and sensing is therefore very tight and precise, using components that have intrinsically high resolution and high

reliability. Longitudinal motion is provided by rotation of the gimbal holding the above components about the optical axis of the telescope. The rotating shaft has the rotary parts of another torque motor and inductosyn mounted to it, again providing the tight control necessary. Drive and error sensing components used for the two drive axes are essentially identical. Control components are optimized for the frequency and control characteristics of each, and logic is developed for the precise control of position in response to a system-level control processor. Figure 5 shows the major elements of the scan control system.

Scan control is initiated by the input proportional commands that set start and end locations of a sounding frame. A location is identified by an inductosyn cycle and increment number within that cycle. Each increment corresponds to 17.5 μradians of mechanical rotation. The increment number determines the value of sine and cosine for that location. The large distance between a present location and the start location is recognized, causing incremental steps (17.5 μrad) at a high rate (10000/s) to reach that location. This occurs simultaneously for each axis.

A complete set of sounding data is taken every 100 ms. The Sounder scanner steps and settles in the fast scan direction (E-W) in 25 ms to less than 1% of a step (2.5 μrad) and then holds within that error for the remainder of the sounding period.

The step angle in the N-S scan is 4X larger than in the E-W scan. Therefore, additional time (one 0.1s sounding period) is used for step and settle only, and its data is invalid. The next sounding period is valid and processed normally.

The Sounder's mirror motion causes spacecraft attitude disturbances which in turn affect the Imager and Sounder pointing (the Imager's mirror creates an equivalent cause and effect relationship). The on-board compensation system reduces this effect to a very low value.

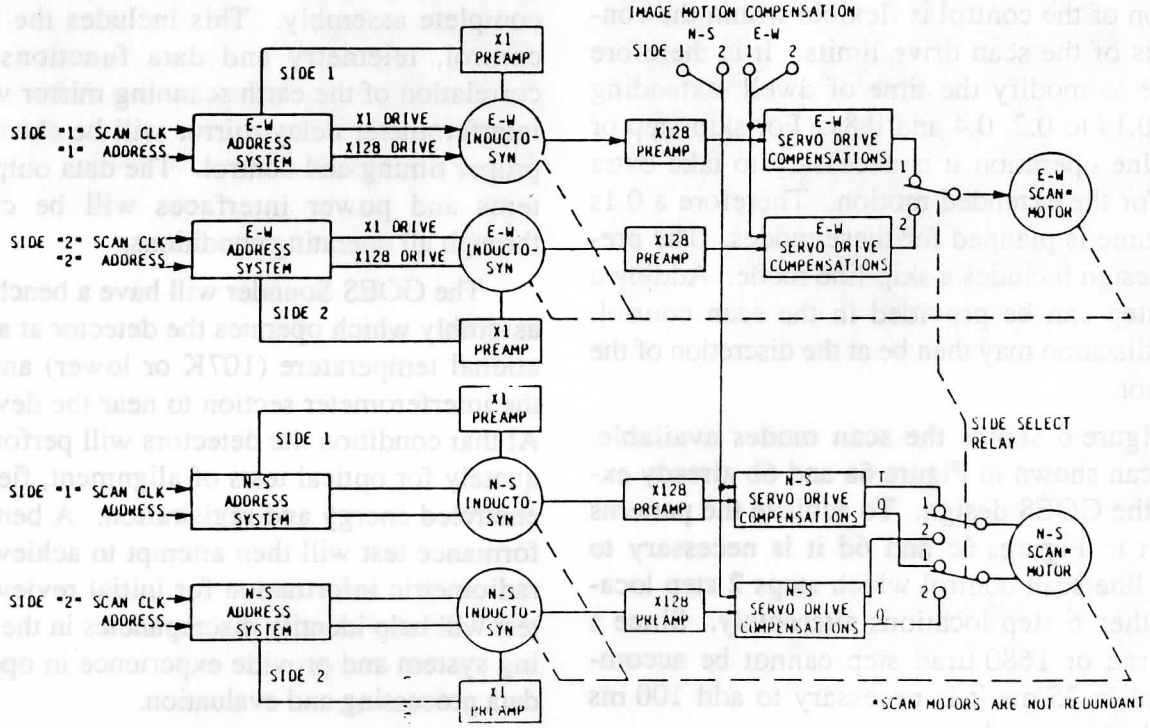

Figure 5. Sounder scan control

Scan to space for space clamp or star sensing or to the IR blackbody uses the slew function. Command inputs (for star sensing or priority frames) or internal subprograms (for space clamp and IR calibration) take place at the proper time during a frame.

The scan control system, shown in Figure 5 is for both the E-W and N-S. The sine and cosine 16-bit codes are latched into their respective multiplying DACs (MDACs). These codes modulate the amplitude of the E-W and N-S carriers. The carriers are in the range of 10 kHz, but are sufficiently different to avoid cross coupling. This error signal from the inductosyn is amplified, bandpass-filtered, synchronously demodulated and fed back to a motor that rotates the inductosyn rotor and mirror to the precise angle specified by the input code.

Scan Patterns for the Interferometer Sounder

The scan control which provides the location signals to the servo system is completely digital, from the four-word instruction from the ground to the software controlled programmer. Modification of the control is flexible within the constraints of the scan drive limits. It is therefore simple to modify the time of dwell, extending from 0.1s to 0.2, 0.4 and 0.8s. For skip-step or skip-line operation it is necessary to take extra time for the extended motion. Therefore a 0.1s dead time is planned for these modes. The present design includes a skip-line mode. Adding a skip-step can be provided in the scan control. The utilization may then be at the discretion of the operator.

Figure 6 shows the scan modes available. The scan shown in Figure 6a and 6b already exist in the GOES design. To achieve the patterns shown in Figures 6c and 6d it is necessary to add a line scan control which steps 2 step locations then 6 step locations alternately. Since a 560 μrad or 1680 μrad step cannot be accomplished in 25 ms it is necessary to add 100 ms to each step period.

As shown in Table 2, the time for coverage of 3000 km E-W by 3000 km N-S is the same for skip step and skip line. Table 3 provides the background information for these calculations. The preferred mode may be determined by selecting uniform area averaging. Increasing the dwell time causes a nearly linear increase in area sounding time.

TEST PLAN

A general test flow plan is shown in Figure 7. A major part of the plan will be dependent upon the interferometer tests which take place at the vendor's location. ITT will supply detectors and optics which are integrated in a test unit to interface to the interferometer under laboratory (bench) conditions. This will permit the vendor to fully check the functional and operational performance of the prime part of the system. These tests are shown occurring in the same general time period as the Sounder subsystem and preliminary system tests.

After delivery to ITT the system will be tested to assure the functional compatibility of the complete assembly. This includes the timing, control, telemetry and data functions. The correlation of the earth scanning mirror with the interferometer delay mirror will be checked for proper timing and control. The data output systems and power interfaces will be checked through all operating conditions.

The GOES Sounder will have a bench cooler assembly which operates the detector at an operational temperature (107K or lower) and cools the interferometer section to near the dew point. At that condition the detectors will perform adequately for optical tests of alignment, field size, encircled energy and registration. A bench performance test will then attempt to achieve some radiometric information for initial review. This test will help identify discrepancies in the operating system and provide experience in operation, data processing and evaluation.

Several total-instrument tests will then be performed, one of which is to detect the presence

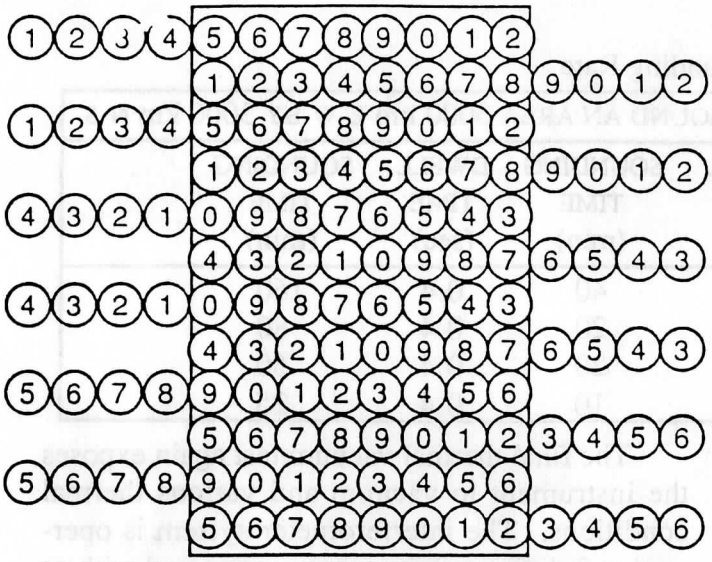

Figure 6a. Single step, normal line

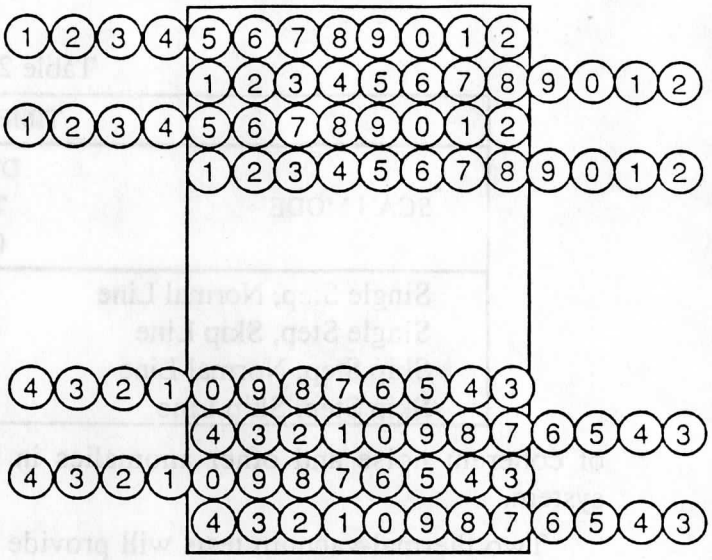

Figure 6b. Single step, skip line

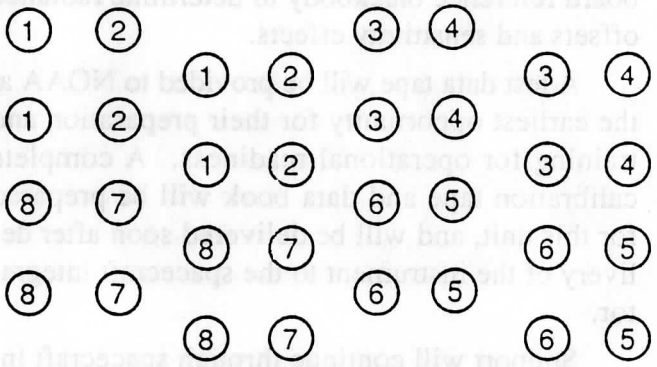

Figure 6c. Skip step, normal line

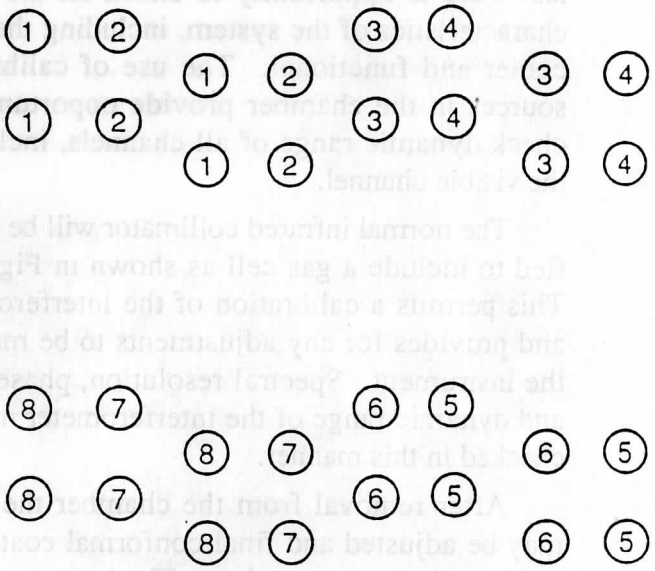

Figure 6d. Skip step, skip line

Figure 6. Sounding in different scan modes (Dwell 0.1, 0.2, 0.4, 0.8s at each location.)

Table 2. Sounding Rate

SCAN MODE	TIME TO SOUND AN AREA 3000 km E-W BY 3000 km N-S			
	DWELL TIME (sec)	SOUNDING TIME (min)	DWELL TIME (sec)	SOUNDING TIME (min)
Single Step, Normal Line	0.1	40	0.4	160
Single Step, Skip Line	0.1	20	0.4	80
Skip Step, Normal Line	0.1	20	0.4	50
Skip Step, Skip Line	0.1	10	0.4	25

of coherent noise and other anomalies in the system.

Two thermal-vacuum tests will provide for preliminary performance analysis prior to vibration and EMI tests, and a final exposure/ calibration test. During the preliminary chamber test there is opportunity to check all the basic characteristics of the system, including thermal, cooler and functional. The use of calibration sources in the chamber provide opportunity to check dynamic range of all channels, including the visible channel.

The normal infrared collimator will be modified to include a gas cell as shown in Figure 8. This permits a calibration of the interferometer and provides for any adjustments to be made to the instrument. Spectral resolution, phase error and dynamic range of the interferometer may be checked in this manner.

After removal from the chamber the gains may be adjusted and final conformal coating or staking of parts put in place. The instrument will then be subjected to the protoflight level vibration test and the same RFI/EMI compatibility and susceptibility tests of the first Sounder.

Following the environmental tests the system is completely checked on the bench for all nonIR performance. The effects on scan location and electrical performance are checked. The visible channel is tested for its final calibration, and the final scan locations are measured.

The final thermal vacuum test again exposes the instrument to vacuum and various thermal conditions. The interferometer system is operated at 3 different base temperatures and with as many as eight different thermal target temperatures as well as a liquid nitrogen cooled "space" target and the on-board reference blackbody. This data is collected, reduced and provided as calibration data to verify performance and provide an initial data base for orbital review. In orbit the system will use deep space and the on-board reference blackbody to determine radiance offsets and sensitivity effects.

A test data tape will be provided to NOAA at the earliest opportunity for their preparation and training for operational readiness. A complete calibration tape and data book will be prepared for this unit, and will be delivered soon after delivery of the instrument to the spacecraft integrator.

Support will continue through spacecraft integration, spacecraft chamber tests and preparation for flight.

The same test flow will be used for the modified Sounder, except that vibration will be limited to acceptance test levels.

A plan for support from the interferometer vendor will provide competent persons at ITT for the installation, operation, test and evaluation of the interferometer, assuring a fully competent test team and a successful integration and test.

Table 3. Sounding Rate Calculations

MODES	STEP	LINE	STEP TIME (SEC)	ADD STEP (SEC)	STEPS PER LINE	TIME/ LINE IN X DIRECTION	LINES	NUMBER OF FOVS (THOU-SANDS)	FRAME TOTAL (SEC)	SPACE +BB (SEC)	TOTAL (SEC)	TOTAL (MIN)
1	Single	Normal	0.1	0	304	30.5	74	90	2257	150	2407	40.1
2	Single	Skip	0.1	0	304	30.5	37	45	1129	80	1209	20.2
3	Skip	Normal	0.1	0.1	76	15.3	74	22.5	1132	80	1212	20.2
4	Skip	Skip	0.1	0.1	76	15.3	37	11.2	566	54	620	10.3
5	Single	Normal	0.4	0	304	121.7	74	90	9005	600	9605	160
6	Single	Skip	0.4	0	304	121.7	37	45	4503	300	4803	80.1
7	Skip	Normal	0.4	0.1	76	38.1	74	22.5	2819	188	3007	50.1
8	Skip	Skip	0.4	0.1	76	38.1	37	11.2	1410	85	1495	24.9
9	Single	Normal	0.8	0	304	243.6	74	90	18034	1200	19234	321
10	Single	Skip	0.8	0	304	243.6	37	5	9017	600	9617	160.3
11	Skip	Normal	0.8	0.1	76	68.4	74	22.5	5069	376	5445	90.8
12	Skip	Skip	0.8	0.1	76	68.4	37	11.2	2535	170	2705	45.1

NOTE:
3000 km E-W scan with 4 overscans is 304 steps.
3000 km N-S scan at 40 km/line is 75 lines but 74 steps.
Space and BB Cal add 80 sec for each 1200 sec of operation.
No time is considered for retrace or star sensing.
Time/Line includes 0.1 sec step time to new line.

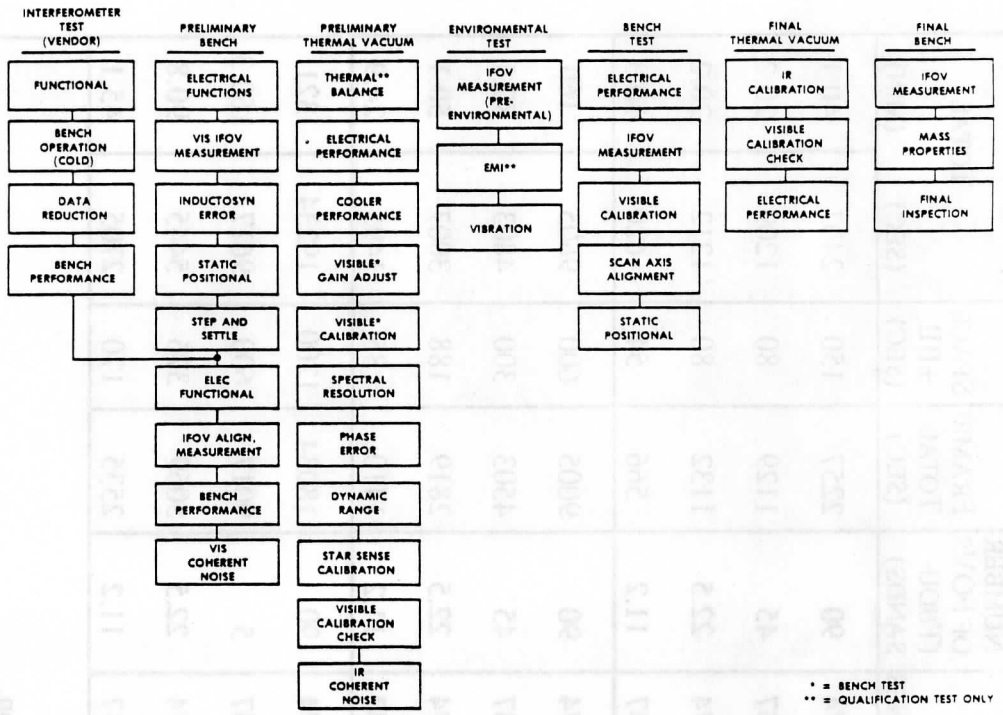

Figure 7. Sounder qualification and acceptance system test plan flow diagram

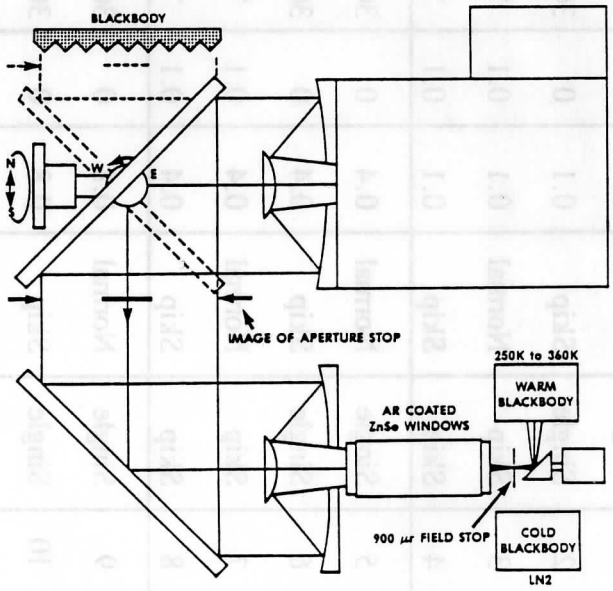

Figure 8. Spectral resolution phase error and dynamic range test

PART III

INTERFEROMETER MODULE DESIGN

(SANTA BARBARA RESEARCH CENTER)

Section 1

INTERFEROMETER SYSTEM OVERVIEW

The details of the engineering design of the interferometer are presented in this part of the report. This section presents an overview of the design, its expected performance, and the ability of the system to obtain accurately calibrated radiometric data. Section 2 provides details on the interferometer optics design and its predicted performance. The electronics design is discussed in Section 3, and the optomechanical design in Section 4.

SYSTEMS LEVEL INSTRUMENT DESCRIPTION

The function of the sounder is to collect terrestrial radiation, which is a superposition of all wavelengths of radiation, both transmitted through, and emitted by, the atmosphere, and to produce a series of digital signals that represent the intensity of that radiation over certain frequency ranges in the infrared and visible portions of the electromagnetic spectrum. The proposed interferometer sounder accomplishes this task by passing the incident radiation through a series of optical elements that transform the spectral information into an optical interference pattern, which is then detected and stored. The stored interference pattern is related to the incident spectrum by the Fourier transform, a procedure that can be performed in real time with the use of on-board digital signal processors. The resulting spectral information is in the form of individual spectral channels, so the entire spectrum can be downlinked.

The main components of the interferometer sounder, as illustrated in Figure 1, are:

Sounder Optics:	Scene mirror and telescope Calibration blackbody Visible System
Interferometer Optics:	Beamsplitter Michelson mirrors (fixed and moving) Dynamic alignment Dichroics for long-, mid- and short-wavelength bands
Aft Optics:	Optical filters Detectors Radiative cooler
On-board Processing:	A/D conversion Fourier transform processor
Downlink:	Command and control Data formatting Spacecraft data bus transfer.

In Figure 1, the components in the dashed box at the left of the figure will be maintained at 290K. Except for the diode pumped laser and ZPD source, these components are those of the existing Sounder design. The components in the dashed box at the right will operate at 220K and represent the interferometer elements to be substituted for the filter-wheel elements. The elements in the dashed box at the top will be able to operate at any of four set points (92K, 97K, 102K, or 107K) and comprise the same elements as in the existing Sounder design, except that the detectors will be replaced by detectors with higher responsivity.

Some of the primary characteristics of the interferometer module are presented in Table 1.

OPERATING MODES

Table 2 presents the characteristics of the interferometer sounder's 12 operating modes. The data rates listed are for telemetry of complex spectra. The rates for the downlink of magnitude spectra would be half these rates.

The spectral resolution modes are defined in terms of OPD travel as shown in Table 3.

Any of the 12 operating modes can be selected by uplinking the proper mode command along with the coordinates of the area to cover. The actual choice of operating mode will depend on whether synoptic or mesoscale information is desired, whether the local cloud conditions are clear, broken, or overcast, and whether skipping 40-km wide E-W lines is acceptable.

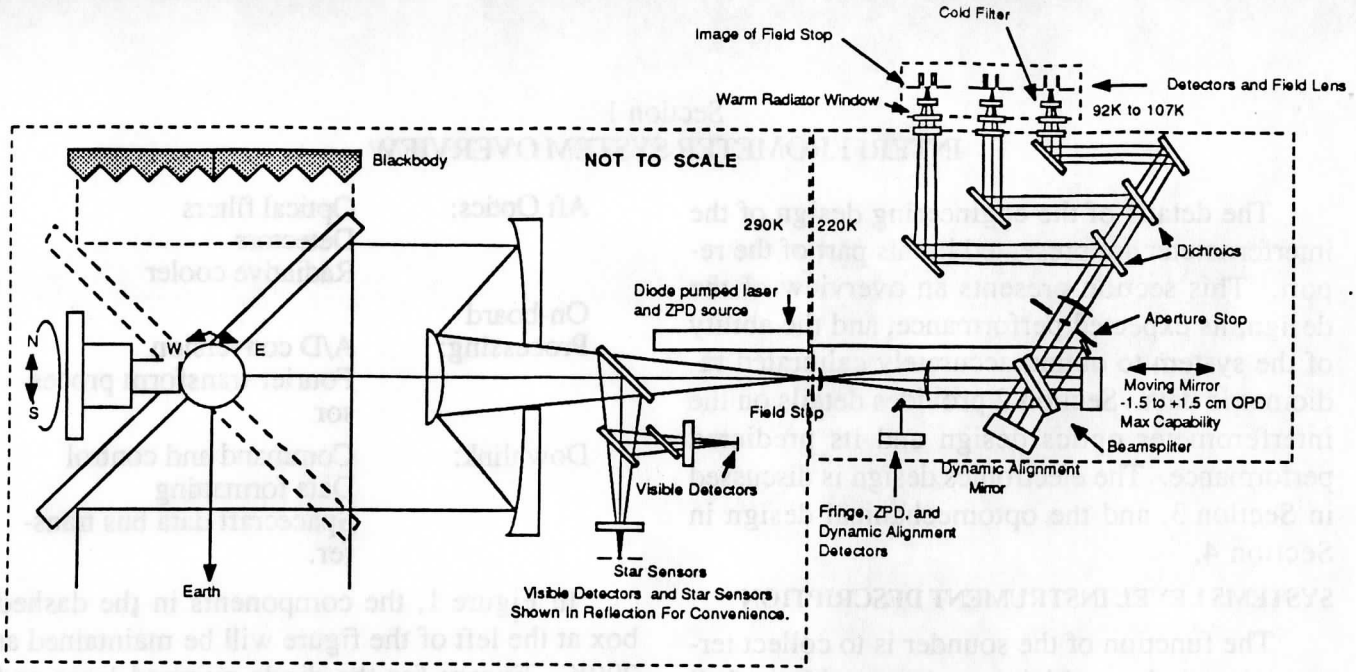

Figure 1. Main components of the interferometer

Table 1. Characteristics of the Interferometer Module

Spectral range (cm^{-1}):	
Band 1	620-1150
Band 2	1210-1740
Band 3	2150-2721
Field of view diameter (mr):	
Telescope	0.242
Interferometer	8.95
	(afocal ratio = 37)
Interferometer:	Auto-aligned plane mirror
Beamsplitter	
Substrate	KBr
Coatings (1/4λ at 3.3 μm)	$Ge+Sb_2S_3$
Maximum double-sided optical path difference (cm):	
Band 1	±1.55
Bands 2 and 3	±0.434
Michelson mirror optical scan rate (cm/s):	4.0
Aperture stop (at exit of interferometer):	
Diameter (cm)	0.84
Area (cm^2)	10.8
Area-solid angle product (cm^2-sr):	4.45×10^{-5}
Detectors:	
Type	HgCdTe (PC in Band 1 and 2, PV in Band 3)
Area (cm^2)	Bands 1 and 2 2.3×10^{-5}
	Band 3 5.8×10^{-5}
Temperatures (K):	
Fore Optics	290
Interferometer	220
Detectors and Aft Optics	92, 97, 102, or 107

Table 2. Characteristics of the Interferometer Sounder's Operating Modes

TIME BETWEEN STEPS (sec)	SPECTRAL RESOLUTION	SCAN PATTERN	COVERAGE (3000 × 3000 km) # FOVs	COVERAGE (3000 × 3000 km) MINUTES	DATA RATE (kbps)
0.1	LOW	1-1	90,000	40	452
		1-2	45,000	20	452
		2*-1	22,500	20	226
		2*-2	11,250	10	226
0.4	MEDIUM	1-1	90,000	160	452
		1-2	45,000	80	452
		2*-1	22,500	50	362
		2*-2	11,250	25	362
0.8	HIGH	1-1	90,000	321	336
		1-2	45,000	170	336
		2*-1	22,500	104	299
		2*-2	11,250	62	299

NOTE: The scene-scan patterns available are 1-1 (single-step, normal line) 1-2 (single-step, skip line), 2*-1 (skip step, normal line), and 2*-2 (skip step, skip line). See Figure 6 of the Part II report for details on these scan patterns.

Table 3. Optical Path Difference Travel for Spectral Resolution Modes

SPECTRAL RESOLUTION	DWELL TIME (sec)	STEP TIME (sec)	TOTAL OPTICAL PATH DIFFERENCE (cm)[a] BAND 1	BAND 2	BAND 3
LOW	0.75	0.1	± 0.150	± 0.108	± 0.108
MEDIUM	3.75	0.4	± 0.750	± 0.434	± 0.434
HIGH	7.75	0.8	± 1.550	± 0.434	± 0.434

[a]The optical path difference for high-resolution Band 1 represents data taking over the full distance of the Michelson mirror travel. The optical path difference for the other bands and modes represent data taking over selected portions of the mirror's travel.

EXPECTED SIGNAL-TO-NOISE PERFORMANCE

In the unmodified design, the energy is directed through a cooled filter wheel, which provides the spectral selection. The proposed modification would replace the relay optics and the filter wheel with a new set of relay optics and an interferometer spectrometer. However, the infrared detectors will be in the same position as in the unmodified design and will provide the same field-of-view capability.

The infrared detectors are arranged in an asymmetric two-by-two array as shown in Figure 2.

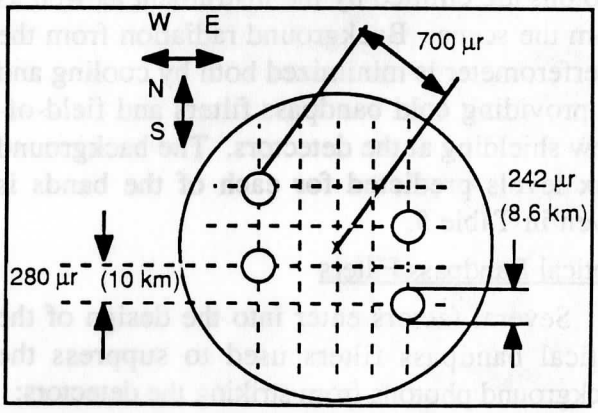

Figure 2. The field of view of the GOES I/M Sounder

One such array is used for each of the three spectral bands. Photoconductive HgCdTe is used for Bands 1 and 2, and photovoltaic HgCdTe is used for Band 3. The Band 1 and Band 2 detectors will be very similar to the detectors developed and flown on the SBRC VAS instruments, but will operate with improved performance due the continuing development of these devices at SBRC. During the Phase B study, the feasibility of using PV HgCdTe for Band 2 will be determined, since these detectors represent a mature technology and are produced routinely at SBRC.

In contrast to the filter-wheel configuration where only one spectral element per detector is integrated at a time, the interferometer configuration integrates all spectral elements at once, resulting in simultaneous acquisition of the spectrum. (This is commonly referred to as the multiplex advantage of the interferometer.)

In the proposed design, the detectors will be cooled to 92K by the GOES I/M radiative cooler for most of the year's operation, but during the high thermal-loading months around the summer solstice, the detectors will operate at 97K or possibly 102K, depending on the orbit. This change in the set point is made so the thermal-noise-limited PC HgCdTe detectors can operate at the lowest possible temperature.

Optical Transmission

To optimize the optical transmission, the number of optical elements is minimized and care is taken in the arrangement of the dichroics. Since some energy is lost passing through a dichroic, the bands requiring the greatest signal strength are reflected first, and the others are passed through. Also folding mirrors are only used when necessary, since each causes some reflection loss and introduces some polarization. The temperature of the three optical assemblies is identified in Figure 1. Table 4 gives the predicted optical transmission and temperature of the optics for each band.

Table 4. Optical Transmission and Temperature for the Optics Assemblies

BAND	FORE OPTICS	OPTICS (290K)	AFT OPTICS (220K)	MARGIN (92K)	TOTAL
1	0.82	0.25	0.73	0.93	0.14
2	0.77	0.21	0.73	0.93	0.11
3	0.77	0.24	0.78	0.93	0.13

Detector Background Radiation

The temperature of the instrument strongly influences the performance of the detectors, since photons are emitted by the instrument as well as from the scene. Background radiation from the interferometer is minimized both by cooling and by providing cold bandpass filters and field-of-view shielding at the detectors. The background flux levels predicted for each of the bands is given in Table 5.

Optical Bandpass Filters

Several factors enter into the design of the optical bandpass filters used to suppress the background photons from striking the detectors:

- The spectral band edges should be in regions of low information content in the observed spectra, because use of dichroics necessitates a small gap in spectral coverage.
- As the bandpass increases, the flux also increases, reducing detector performance overall, but especially at the short wavelength end of the optical band.
- An appropriate choice of the optical bandpass filters can reduce the effects of detector nonlinearity on the spectra.

In the light of these considerations, the bandpass of the optical filters is 4% larger than the bandpass defined for each of the bands.

System Signal-To-Noise Performance Summary

The performance of an interferometer is evaluated on the basis of its noise equivalent spectral radiance (NEN) as follows:

Table 5. Estimated Background Radiation

BAND	EXPECTED SCENE RADIANCE (MODULATED) (photons/sec-cm^2)	BACKGROUND RADIANCE (UNMODULATED) (photons/sec-cm^2)
1	7.05×10^{16}	1.85×10^{17}
2	4.95×10^{15}	1.55×10^{16}
3	7.65×10^{13}	1.35×10^{14}

$$NEN_{unapodized} = \frac{\sqrt{A_d \cdot \frac{1}{2 \cdot T_i}} \cdot X \cdot \sqrt{2} \cdot 10^7}{A_o \cdot \Omega_{fov} \cdot t_o \cdot D^*} \left[\frac{mW}{m^2\ sr\ cm^{-1}}\right]$$

where:

A_d = The area of the detector [cm^2]

T_i = The integration time per scene [sec]

A_o = The area of the optics aperture [cm^2]

t_o = The overall optical system transmission

D^* = The detectivity of the detector elements $\left[\frac{cm\sqrt{Hz}}{W}\right]$

X = The single sided optical path difference [cm]

Note: $\Delta\upsilon = \frac{1}{2X} \cong$ The unapodized spectral resolution [cm^{-1}]. (As defined by UW for this contract.)

Table 6 summarizes the spectral characteristics of the bandpass optical filters.

Table 6. Optical Filter Wavelength Characteristics

BAND	SHORT WAVE-LENGTH CUTOFF (μm)	LONG WAVE-LENGTH CUTOFF (μm)
1	8.52	16.45
2	5.63	8.43
3	3.60	4.74

The expected performance can be calculated using the summary of instrument parameters given in Table 7.

Table 7. Summary of Instrument Parameters Used in Calculating NEN

BAND	A_d (cm^2)	T_i (sec)	X (cm)	AΩ (cm^{2}sr)	t_o	D* (cm$\sqrt{Hz}$/W)
1	2.3×10^{-5}	0.125	0.25	4.5×10^{-5}	0.14	3.7×10^{10}
2	2.3×10^{-5}	0.125	0.25	4.5×10^{-5}	0.11	9.0×10^{10}
3	5.8×10^{-5}	0.125	0.25	4.5×10^{-5}	0.12	1.2×10^{12}

The specified, desired, and expected performance are presented in Table 8. The Table 8 performance estimate is for a 2 cm^{-1} unapodized spectrum and 0.125 second integration time. Note that the NENs for soundings will be better than those shown in Table 8 by a factor of the square root of the number of clear FOVs per sounding. With the addition of new temperature set points to account for seasonal temperature variations, the cooling provided by the existing passive cooler will result in performance that exceeds the specified performance in all bands and that exceeds the desired performance in the critical Band 1.

Table 8. Predicted NEN Performance

	NEN (mW/m^2-sr-cm^{-1})		
BAND	SPECIFIED	DESIRED	EXPECTED
1	0.44	0.2	0.145
2	0.12	0.04	0.076
3	0.01	0.0035	0.0084

As shown in Table 9, The interferometer will have significantly better NENs than the existing filter-wheel sounder, if we compare bands with the same wavenumber and spectral resolution. For this comparison, the D* was calculated for each of the NOAA channels at a step time of 0.1 second, and the interferometer data were

aggregated up into the spectrally broader NOAA bandwidths. The aggregation represents a simple square root of the ratio of the resolution elements:

$$NEN_{NOAA} = NEN_{interferometer} \cdot \sqrt{(\Delta\nu_{interferometer}/\Delta\nu_{NOAA}}$$

This improvement is a direct consequence of the multiplex advantage of the interferometer over the filter-wheel radiometer.

The requirements for these channels are from Ford Specification No. 565054 Rev A Section 3.2.1.

Table 9. Expected NEN of Synthesized NOAA Channels

Channel Number	Center Wavenumber	Resolution $\Delta\upsilon$	NEN Specified	NEN Desired	NEN Expected
1	680	13	0.66	0.25	0.065
2	696	13	0.58	0.25	0.066
3	711	13	0.54	0.25	0.067
4	733	16	0.45	0.25	0.063
5	748	30	0.44	0.2	0.047
6	790	50	0.25	0.15	0.038
7	832	50	0.16	0.06	0.040
8	907	25	0.16	0.06	0.062
9	1035	25	0.35	0.12	0.071
10	1345	55	0.16	0.05	0.017
11	1425	80	0.12	0.04	0.015
12	1535	60	0.15	0.04	0.018
13	2188	23	0.013	0.004	0.0029
14	2210	23	0.013	0.004	0.0030
15	2245	23	0.013	0.004	0.0030
16	2420	40	0.008	0.003	0.0025
17	2513	40	0.0082	0.003	0.0025
18	2671	100	0.0036	0.002	0.0017

DYNAMIC RANGE

The maximum signal-to-noise ratio (SNR) presented to the A/D converters determines the dynamic range that must be accommodated. The maximum SNR will occur when the instrument is looking at hot and dry regions of the earth. The SNR was calculated, then multiplied by a factor of two to ensure that the instrument would not be quantization noise limited. Using the above criteria, the number of bits required for Band 1, Band 2, and Band 3 are 14, 13, and 12, respectively. This is an internal bit requirement; the output spectral channels are all digitized to 12 bits.

DETECTOR PERFORMANCE

Using the total background levels given in Table 5, the ultimate performance (BLIP) of the detectors was calculated, and the results are presented in Table 10. With high background levels and cold detectors, photon flux noise would be expected to dominate. However, the performance of Bands 1 and 2 are limited instead by detector thermal noise, although photon noise is not negligible in Band 2. Band 3 is fully photon noise limited.

Table 10. Predicted D* Detector Performance at 92K

BAND	D* AT MID-BAND (cm (Hz)$^{1/2}$/W)	% OF BLIP
1	3.65×10^{10}	54
2	8.95×10^{10}	68
3	1.15×10^{12}	100

Table 11 gives the detector performance expected at the three operating set points.

Table 11. Predicted Detector Performance at Operating Set Points

TEMPERATURE (K)	D* (cm (Hz)$^{1/2}$/W) BAND 1 ($\times 10^{10}$)	BAND 2 ($\times 10^{10}$)	BAND 3 ($\times 10^{12}$)
92	3.7	9.0	1.2
97	2.5	7.5	1.1
102	1.9	5.9	1.1

EXPECTED CALIBRATION PERFORMANCE

The design of the proposed interferometer sounder takes into account the need for high absolute calibration accuracy. The HIS aircraft instrument data has shown that the calibration accuracy for a properly designed interferometer spectrometer is limited by the same factors as a filter-wheel radiometer. These factors (the knowledge of the reference source temperature and emissivity and the linearity of the detectors and electronics) are essentially the same for the interferometer version of GOES as for the filter-wheel radiometer version. However, although the radiometric accuracy is the same, the spectral calibration accuracy of the interferometer is vastly superior.

LASER CHARACTERISTICS, LIFETIME, AND RELIABILITY

Calibration of the interferometer is based on an accurate knowledge of the position of the moving mirror, and its position is monitored by a separate part of the laser-illuminated interferometer. The laser system of choice for the GOES Sounder modification is a laser-diode, pumped Nd:YAG laser that operates at 1.06 μm. The laser will be single frequency and have an operational lifetime of 7 years. The weight of the laser, mount, and electronics will be less than 0.4 pounds.

Interferometer systems such as ATMOS, that use a HeNe gas-discharge laser, require high-voltage power supplies; and both the power supply and the discharge tube have reliability problems that cause them to be inappropriate for the 5-10 year GOES mission. Flashlamp-pumped solid-state lasers would reduce the voltage requirements, but flashlamp lifetime is also limited.

The GOES instrument will use an all-solid-state laser system, illustrated schematically in Figure 3, employing a diode laser to longitudinally pump a Nd:YAG laser rod for a low-power (2 mW) CW output. This laser system is commercially available from at least four companies in the United States (McDonnell-Douglas, Spectra Diode Laboratories, Spectra Physics, and Amoco Laser Company). McDonnell-Douglas has a contract to deliver several space-qualified, 5-10 year lifetime diode-pumped lasers to the U.S. Air Force in the fourth quarter of 1988. By using diode lasers to optically pump the Nd:YAG rods, only low-voltage (a few volts) power supplies are needed, thus eliminating the need for special environmental considerations to avoid arcing in space.

The position calibration laser requires an output power of only 2 mW. This is well below any of the damage threshold mechanisms for Nd:YAG -- with lifetimes projected in the tens to hundreds of years. As for the diode laser pumps, because of the relatively high conversion efficiency (over 10% in the end-pumped scheme), only 20 mW is required. As indicated in Table 12, which shows the projected lifetimes of various state-of-the art diode lasers as a function of technological maturity and operating temperature, existing space-qualified diode lasers with this power capability will have lifetimes of more than 20 years; and when operated at the 15°C temperature proposed for GOES, these lasers will operate even longer. However, in order to avoid the possibility of a single-point failure, the Nd:YAG laser rod will be designed to receive redundant pump-diode emission using an already established technique.

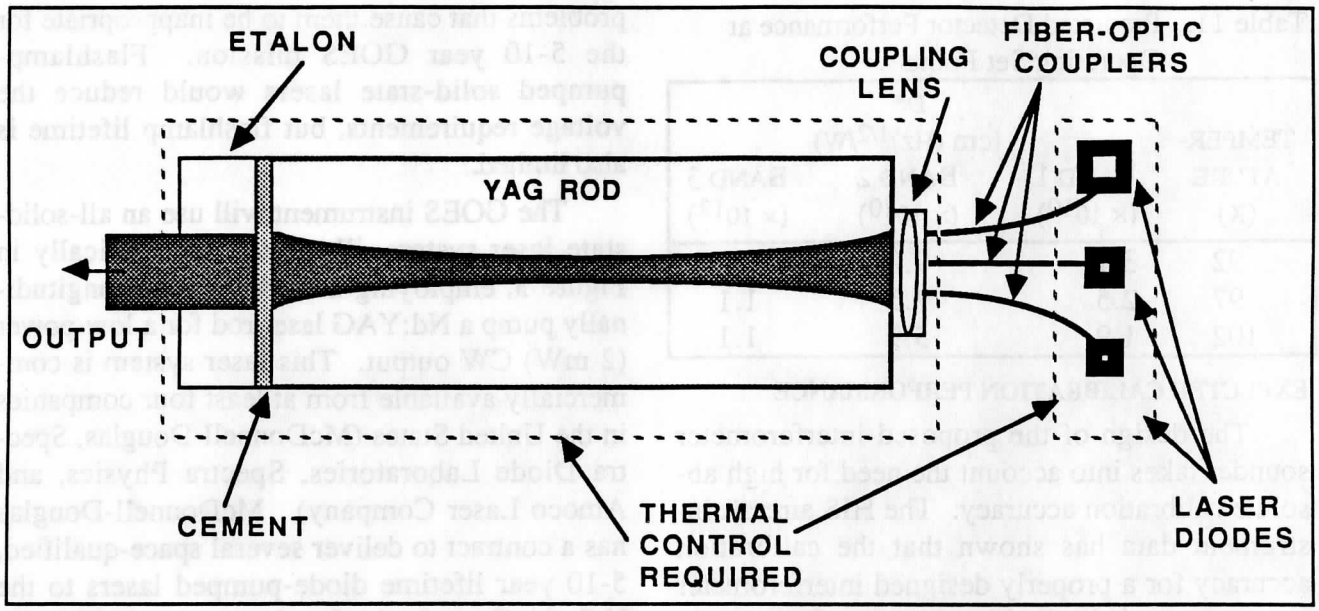

Figure 3. Schematic of the laser proposed for GOES

Table 12. Historical Lifetime Data: Spectra Diode Labs' Diode Lasers

CW Power (mW)	Year	Median Life (Years) at: 30°C	15°C
28*	1987	80	320
500	1987	10	40
100	1986	20	80
100	1984	3	12

* Space-qualified

Diode-pumped Nd:YAG lasers now being produced to operate in a single transverse (spatial) mode as well as a single longitudinal (frequency) mode. The single longitudinal mode is maintained with the introduction of an etalon into the Nd:YAG laser cavity. Nd:YAG lasers have been operated successfully in an environment of high radiation and are mechanically stable. Properly packaged, the combination of the diode laser and Nd:YAG laser rod is the most rugged laser system currently available. Since it is more rugged than the HeNe laser used in ATMOS (which successfully withstood Shuttle launch vibrations), this all-solid-state system is expected to result in a major advance in spaceborne reliability.

Section 2

INTERFEROMETER OPTICS DESIGN

The optical system for the proposed GOES Sounder Interferometer consists of three basic subsystems: the ITT fore optics (pointing optics and collecting telescope), the interferometer optics, and the condenser lens/detector assembly. This section describes how the interferometer optics and related condenser lens/detector assembly have been successfully designed to use the existing Sounder fore optics. The section concludes with a discussion of some important manufacturing considerations.

SOUNDER OPTICS

The filter-wheel sounder has a 31.1 cm aperture telescope that views the earth, space, or the on-board calibration blackbody, depending on the scene mirror scan angle. A sun shade and baffles are used to minimize the optical and radiometric influence of solar radiation on the fore optics. These features also meet the requirements of the interferometric design.

Just aft of the telescope there is a folding mirror that separates the visible wavelengths from the infrared energy. The visible energy is directed to star sensing detectors and to detectors for the visible channels. This visible system does not need to be modified to incorporate the interferometer.

The remaining infrared wavelengths enter the interferometer optics; this system will be described in the following subsections.

In summary, the fore optics assembly used for the filter-wheel sounder, from the scene scan mirror through the visible and star-sensor dichroics, would be retained in an unmodified form for the interferometer sounder.

INTERFEROMETER OPTICS

The optical configuration, shown in Figure 4, is primarily reflective to avoid restricting wavelength coverage. As indicated by Figure 5, it achieves the basic performance goals and can be packaged to fit into the existing space.

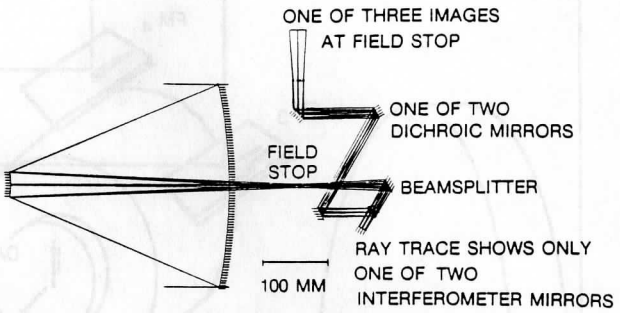

Figure 4. Ray trace of optical configuration

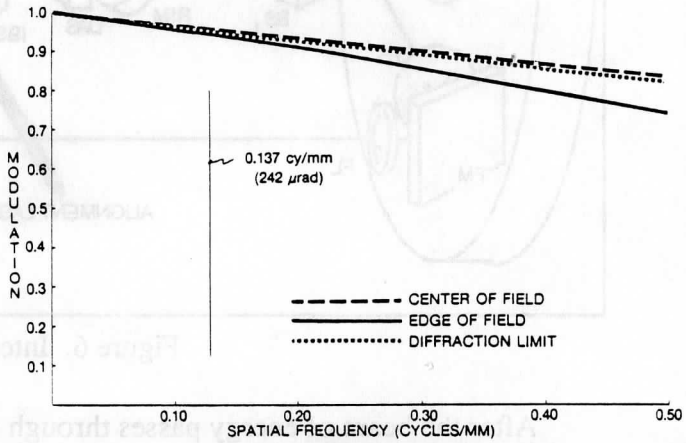

Figure 5. Predicted optical performance

A preliminary layout was established and potential imaging problems analyzed by computer ray tracing. A brief description of the function of each of the elements in the design follows.

As shown in Figure 6, the beam of energy enters the interferometer cavity through the center of the existing telescope primary mirror. The light emerging from the telescope is recollimated, passed through the interferometer, and then imaged at the face of a condenser lens, which directs the energy onto the detectors. Additional folding mirrors, stops, and beamsplitters are included for packaging purposes and to improve the performance of the instrument.

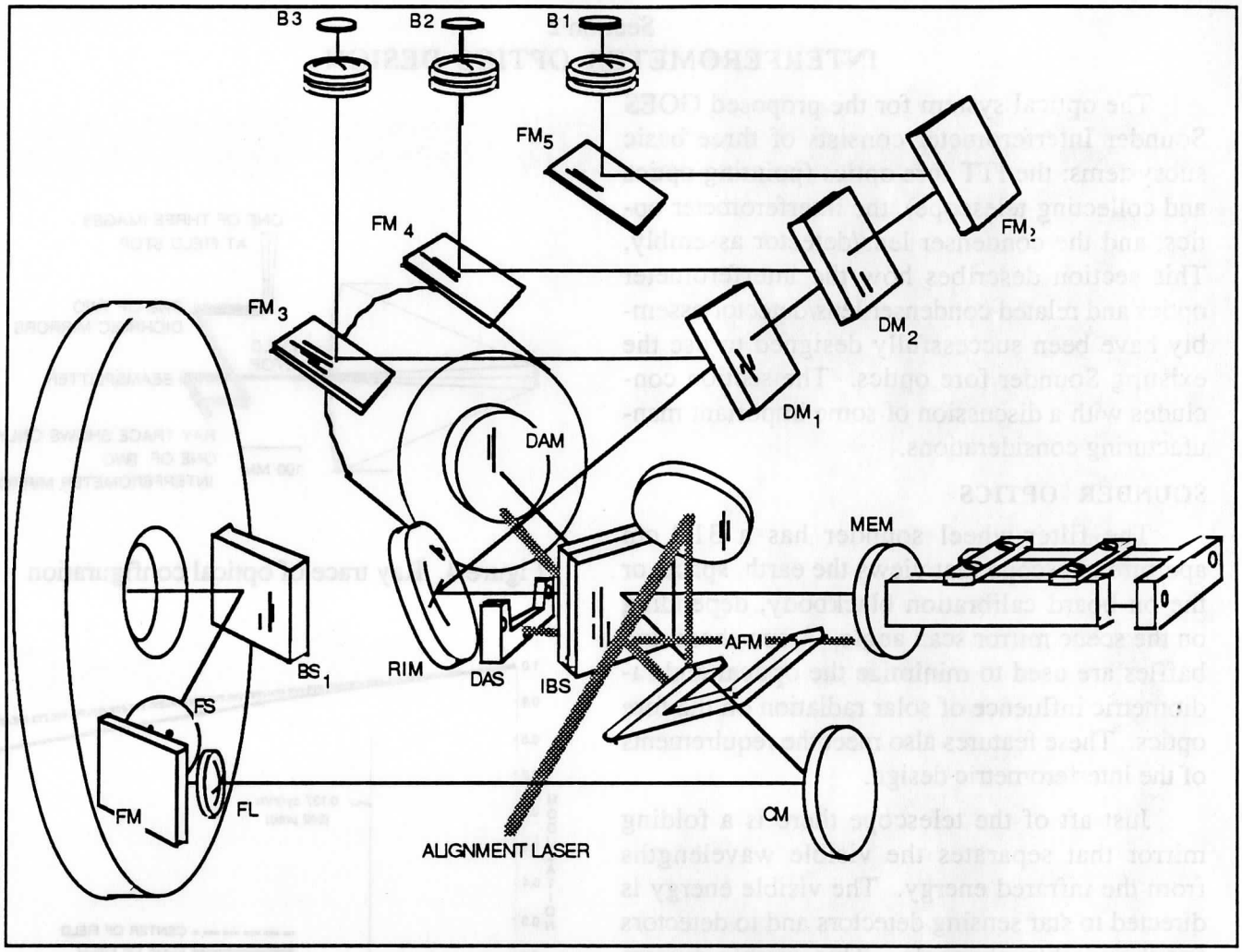

Figure 6. Interferometer optics layout

After the beam of energy passes through the center of the primary mirror, the following components are encountered:

- A dichroic folding mirror (BS1) separates the visible wavelengths from the infrared energy. The path of the visible wavelengths is not shown in Figure 6, and treatment of these wavelengths was not considered in the study.
- The system field stop (FS) is placed in the optical beam, which contains all three infrared channels, thereby ensuring band registration. The field size and orientation are the same as the current ITT design; four, 242 mr apertures are oriented so as to provide four parallel scan lines as the Sounder's scan mirror scans from east to west.
- A folding mirror (FM1) is then placed in the path of the beams to keep the dimensions of the assembly within packaging constraints.
- The field lens (FL) is used to reimage the aperture of the telescope at the output side of the interferometer beamsplitter. The true, limiting aperture stop (not shown) is located at the output of the beamsplitter to ensure that radiation originating at the aperture stop is not modulated by the moving Michelson mirror.
- The output of the field lens is sent through a collimating mirror (CM); an off-axis parabola.
- The scene energy and the laser beam enter the Michelson interferometer, which is composed of the interferometer beamsplitter (IBS), the moving Michelson mirror (MEM),

and the fixed Michelson mirror used for dynamic alignment (DAM). The alignment folding mirror (AFM) redirects the laser beam for the dynamic alignment mechanism so it is parallel to the scene radiation path.

- The interferometer beamsplitter (IBS) and compensator are made of KBr to provide adequate transmission of the long wavelengths. Both KCl and KBr are acceptable materials; KBr has superior long-wavelength transmission, while KCl has better moisture resistance. This element might be considered a manufacturing concern because the coating is critical and the material is sensitive to moisture damage. However, KCl was used successfully in the HIS instrument. The final selection of the beamsplitter material will occur during the Phase B or C studies.
- The Moving Michelson Mirror (MEM) is supported on a flex-pivot mechanism that provides uniform motion through the range of mirror travel. The flex pivots eliminate the roughness and wear associated with ball bearings.
- Upon exiting the interferometer, the scene radiance is reimaged. An off-axis parabola is employed as the reimaging mirror (RIM). Orientation is chosen so that the optical axis of the system is folded to position the remaining elements in a plane, allowing easy entrance into the radiative cooler.
- The first dichroic mirror (DM1) is positioned at 30° to the optical axis to separate Band 3 (2150 to 2721 cm^{-1}) from the other bands by means of reflection. The second dichroic element (DM2) separates Band 2 (1210 to 1740 cm^{-1}) from Band 1 (620 to 1150 cm^{-1}).
- Four folding mirrors, (FM2), (FM3), (FM4), and (FM5) are used to direct the optical beams onto windows in the radiative cooler containing the cold detectors.

AFT OPTICS

Scene energy entering the long-wavelength, mid-wavelength, and short-wavelength radiator windows passes through a set of condenser lenses. The condenser lenses, employed to image the aperture stop onto the detectors, must be highly convergent to keep the detector size as small as possible. In addition to the condenser lenses, the radiance passes through cold optical filters that are optimized for each spectral band and used to reduce the effects of background radiation. Finally, the focused scene energy from the three wavelength intervals is converted by the cooled detectors into analog electrical signals, preamplified, and passed onto the digital processing system.

DYNAMIC ALIGNMENT

The suspension for the dynamic alignment mirror (DAM) is driven by a feedback loop to compensate for misalignment with the moving Michelson mirror. This mechanism is the unique feature of our design that will permit satisfactory interferometer performance despite environmental changes that will alter the mechanical alignment. This is a well-proven approach in many field applications, including the HIS aircraft instrument.

Upon exiting the interferometer, the alignment laser beam is directed to a set of optical interference fringe detectors that detect slight deviations in the relative alignment of the moving and fixed Michelson mirrors. Signals from the detectors are used by the dynamic alignment control system to adjust the fixed-mirror orientation to correct the misalignment.

MANUFACTURING CONSIDERATIONS

Image Quality

The angular diameter of the system field stop is 242 mr. Achieving a sharp image across this field will not be difficult. The optical system convergence is f/12 at the telescope's prime focus and f/42 at the reimaged field. The "slow" optics permit the geometrical image errors to be easily controlled. However, there are two design concerns in the imaging task. First is the condenser lens, which operates at a small f/#, and second is the effect of diffraction on image quality.

The condenser lens is employed to image the aperture stop on the detector. It is important, especially at long wavelengths, to keep the

detector size as small as possible. This leads to a condenser design for a convergent cone faster than f/1. If the design employed by ITT were to be adopted, there would be no allowance for tolerance on the detector size.

The effect of diffraction on image quality will be discussed in more detail in the following subsection.

We have assumed there are alignment adjustments that will permit correcting for all manufacturing irregularities and that the aperture will be totally imaged on each detector. However, it is not clear that the alignment will be held accurately enough after environmental changes. An in-depth tolerance analysis will be required to show the radiometric effects of environmental variations.

Beamsplitter Properties

The KBr interferometer beamsplitter will be similar to the one used in the HIS aircraft flights and also to those commonly used by Bomem, Inc. KCl and KBr have very similar physical properties, but KBr is the more commonly used material. Since the interferometer assembly will be enclosed in a hermetically sealed structure to enable cooling of the entire assembly, the assembly surroundings can be gas filled or evacuated to prevent moisture damage to the beamsplitter.

Two dichroic beamsplitters are used to separate the optical path into three spectral bands. These beamsplitters present no technological challenges.

DIFFRACTION EFFECTS

The GOES L/M instrument will operate at wavelengths out to 16 μm where the commonly noted diffraction effects are blurred field edges. The relayed image essentially puts an additional stop in the optical path, leading to energy losses. In order to better understand the nature and magnitude of these losses, a detailed analysis was undertaken by Hughes Electro-Optical and Data Systems Group (EDSG). It should be noted that these effects are not specific to an interferometer instrument; the same diffraction effects exist with filter-wheel instruments.

The functional illustration of the optical system, shown in Figure 7, reveals the nature of the diffraction issue. There is a field stop, 0.9 mm in diameter, at the prime focal plane, while the diameter of the central diffraction ring due to the telescope aperture is 0.29 mm (for 10 μm wavelengths). In addition, at the aperture stop the central diffraction ring due to the field stop is 2.71 mm in diameter, while the diameter of the aperture stop is only 8.4 mm. This could result in spreading a significant portion of the optical

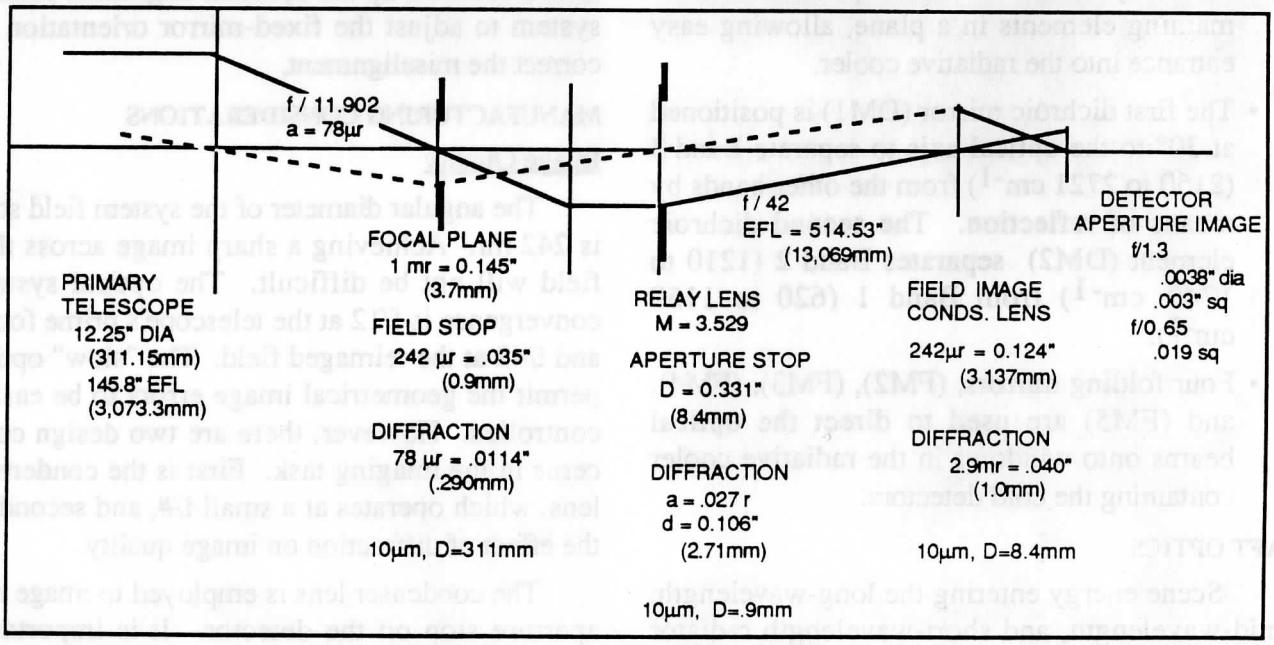

Figure 7. Optical relationships for the sounder

beam outside the physical stop. These losses, along with similar diffraction conditions at the condenser lens and the detector plane make it difficult to image the aperture sharply on the detector. Each of these cascading diffraction effects serves to reduce the energy throughput of the optical system.

EDSG determined the diffraction behavior of the system using the System Optical Quality (SOQ) code. In this approach the normalized power throughput of the system is determined by measuring the power throughput due to a point-source object as a function of field angle. At each aperture and stop in the system, the associated diffraction and limiting of the beam was calculated, and the resulting transmitted beam was propagated to the next aperture. These losses (as a function of the point-source field angle) were used to determine the cumulative power throughput at the field stop, aperture stop, condenser lens, and detector. These results are shown in Figure 8 using a wavelength of 16 μm. These curves represent the throughput losses for a single radial slice through the field of view.

In order to extend these results over the full field of view of an extended source, the results corresponding to the detector curve were integrated and normalized over the area of the detector. This function of transmitted power vs. field angle at the detector plane is shown in Figure 9. Using standard integration techniques, the normalized power throughput for a 0.0038-inch detector at a wavelength of 16 μm was calculated to be roughly 70% for this optical system. However, it should be noted that this analysis was performed for an unobscured system; additional losses due to obscuration can be expected.

This generalized diffraction analysis shows that, although diffraction losses are present in this optical system, they do not degrade optical throughput significantly. A further analysis of this system might include optical throughput and diffraction dependence on the aperture positions and sizes in order to minimize losses. The result of this analysis has been an improved understanding of the detailed optical transmission of the interferometer system and a confirmation of the integrity of the proposed optical design.

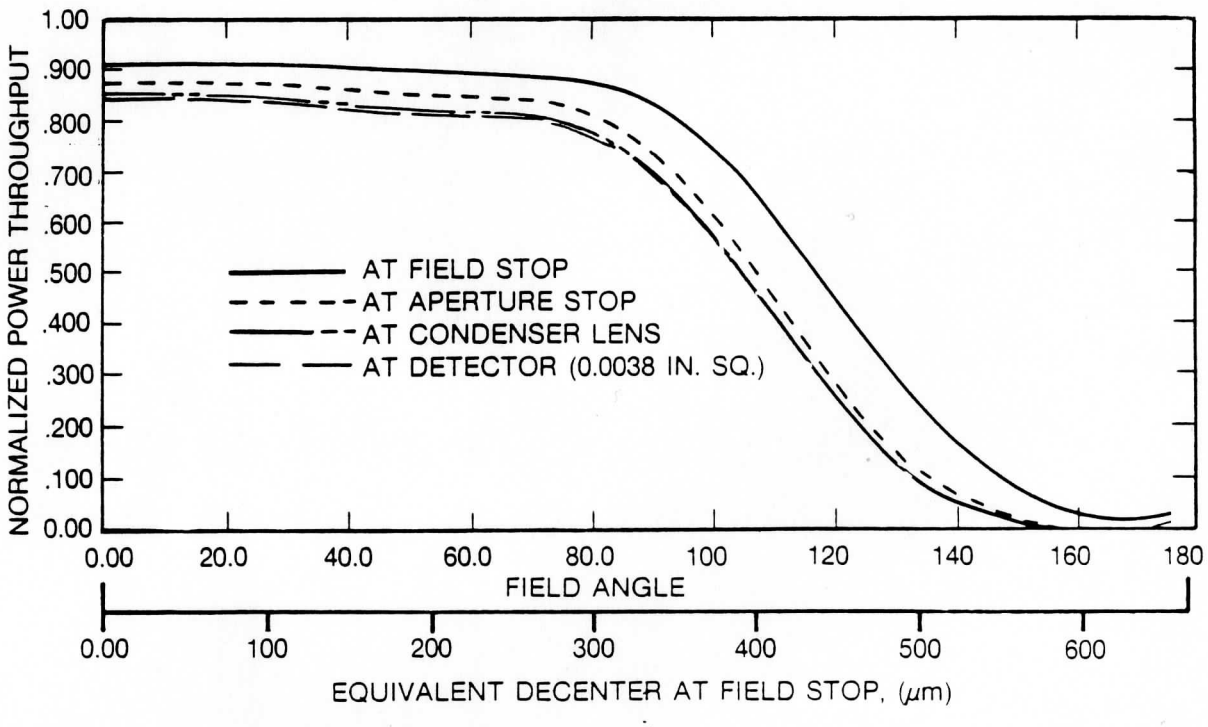

Figure 8. Point-source power throughput versus field angle for the GOES I/M Sounder

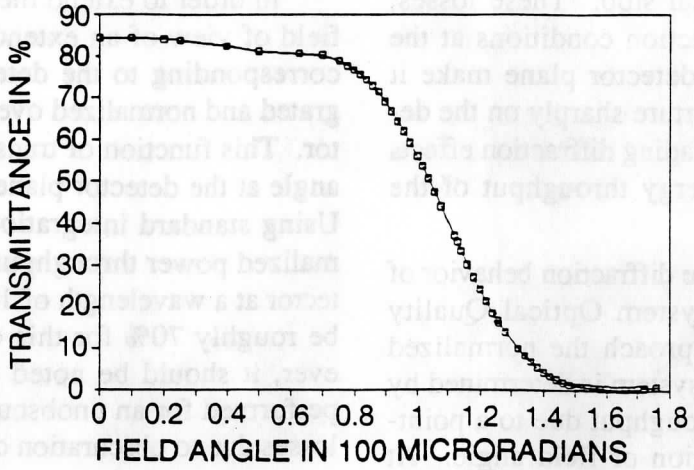

Figure 9. Optical transmittance

Section 3

INTERFEROMETER ELECTRONICS

At the onset of this section, system functional requirements for the interferometer sounder are stated. Subsequently, a conceptual design meeting those requirements is discussed in detail. Then, an in-depth view of the necessary analog electronics, digital signal processing, and control systems is given, and, finally, a list of necessary electronic parts requiring GOES program approval is summarized.

FUNCTIONAL REQUIREMENTS

The following electronics functional requirements will be discussed: spectral resolutions of the interferometer sounder data-taking modes, Michelson mirror control requirements, dynamic alignment system requirements, data sampling rate, and digital signal processing.

Data Taking Modes

As discussed in Section 1, the interferometer sounder has the capability of acquiring data at low, medium, or high spectral resolution. The optical-path-difference range and the time between scene mirror steps, which together define the spectral resolution and instrument performance, are given in Table 13.

As indicated previously, the actual data-taking modes are a combination of the scene scan pattern and the dwell time used. The scene scan pattern can be specified independently of the dwell time; however, in the current design, once the dwell time is chosen, the spectral resolution is fixed.

Michelson Mirror Motion Control Requirements

The Michelson moving mirror motion control requirements for each of the three spectral resolutions are:

- Travel extent control for each spectral resolution.
- Motion-control accuracy of 1 - 2%.
- Michelson mirror motion synchronization with pointing mirror motion
- Command and control module interface.

Dynamic Alignment System

An alignment system is required to maintain alignment of the optical elements over time, due to environmental changes. In a Michelson interferometer, the only fringe patterns of interest are those due to optical path differences between the optical path to and from the fixed mirror and the optical path to and from the moving mirror. This means that the fringes caused by slight angular misalignment of the fixed mirror surface relative to the moving mirror surface must be avoided. These unwanted fringes are eliminated by using the Bomem-developed dynamic alignment concept. It consists of a controller and alignment actuators for rotating the fixed mirror around the x-y axes to maintain optical alignment between the fixed mirror and the moving mirror while the moving mirror is in motion. In addition, an interface with the command and control module performs an alignment search to find alignment on startup or if alignment is lost.

Data Sampling Rate

As discussed previously, there are 4 detectors in the focal plane of each of the 3 bands, resulting in a total of 12 detector channels. The laser wavelength of 1.06 μm results in a total of 9434 wavelengths per centimeter, or an opportunity to collect up to 9434 samples/cm. Thus, at the Michelson mirror's optical scan rate of

Table 13. Characteristics Of The Three Spectral Resolutions

SPECTRAL RESOLUTION	DWELL TIME (sec)	TIME PER STEP (sec)	TOTAL OPTICAL PATH DIFFERENCE (cm) BAND 1	BAND 2	BAND 3
LOW	0.075	0.1	± 0.150	± 0.108	± 0.108
MEDIUM	0.375	0.4	± 0.750	± 0.434	± 0.434
HIGH	0.775	0.8	± 1.550	± 0.434	± 0.434

4.00 cm/s, samples can be taken every 26.5 μs. This is the data sample rate selected for Bands 2 and 3, but Band 1 samples are taken on every other cycle to reduce the A/D Converter sample rate.

Signal Processing

We plan to perform the transformation from interferogram to spectra on board, downlinking the spectral data and using data compression if necessary. The data rate in each band for this case is computed from:

$$\text{RATE} = (\#\ \text{FOVs/step}) \times (\#\ \text{spectral channels}) \times (12\ \text{bits/channel})/(\text{time/step}).$$

The total data rates, summing over Bands 1, 2, and 3, are presented in Table 14. The higher rate corresponds to the transmission of complex spectra, the lower rate applies if magnitude spectra are sent to the ground. Note that all data rates to send down the full spectra are less than 500 kbps.

Table 14. Data Rates For The GOES Interferometer By Operational Mode

SPECTRAL RESOLUTION	TOTAL DATE RATE (kbps) SINGLE STEP MODE	SKIP-STEP MODE
LOW	452 / 226	226 / 113
MEDIUM	452 / 226	362 / 181
HIGH	336 / 168	299 / 149

CONCEPTUAL DESIGN OVERVIEW

The conceptual design that evolved for the electronics was derived as much as possible from the Thermal Emission Spectrometer (TES) design for the Mars Observer spacecraft. The TES interferometer is similar to the interferometer proposed for the Sounder in many ways and represents a mature design. Both interferometer systems are intended for meteorology missions. Although the TES is designed primarily for geological applications on the Mars Observer spacecraft, it will also be used to study the Martian atmosphere and weather systems. Both systems feature a Michelson mirror control system, with temperature control of critical system elements. Both have high accuracy requirements and are required to have high reliability and long lifetimes, including some system redundancy.

The electronics block diagram for the point design GOES L/M Sounder modified to incorporate an interferometer is presented in Figure 10 and shows the interrelationships among the various system elements. On the left side of the diagram is the ITT optical system with its scan mirror and telescope system. Scene energy travels through the field stop to the sounder's beamsplitter where the energy is reflected towards the alignment mirror and passed through to the Michelson scan mirror. It is then reflected back to the beamsplitter, to a folding mirror, and through dichroics to the detector arrays.

Each detector output is passed first to the four preamplifiers directly above them, i.e., one preamplifier per detector. The preamplifiers supply the bias requirements to the detectors and provide gain and initial output signal band shaping. As shown, the preamplifier output passes through the amplifier and Bessel filters, which provide the required gain and bandwidth filtering for optimizing the signal-to-noise ratio. At this point there is still one analog channel per detector. The detectors and preamplifiers will be modified versions of the ITT system.

The output of each analog channel continues to one of two sample-and-hold (S/H) amplifiers and to one of two analog-to-digital (A/D) converters. Only one S/H and A/D pair is active; the other is redundant. All the remaining elements in the diagram, except for the fringe and alignment detectors, are also redundant.

As will be shown, three DSP modules are required to process the three bands. The DSP applies a fast Fourier transform to the interferograms to create the spectral data.

The output of the DSP goes to the First-In First-Out (FIFO) memory buffer. The FIFO memory queues the output data, smoothing the data flow over time, thus minimizing transmission rate peaks. The FIFO output is fed to the ITT command and data bus. Commands from the data bus are accepted and processed by the command and control module (CCM).

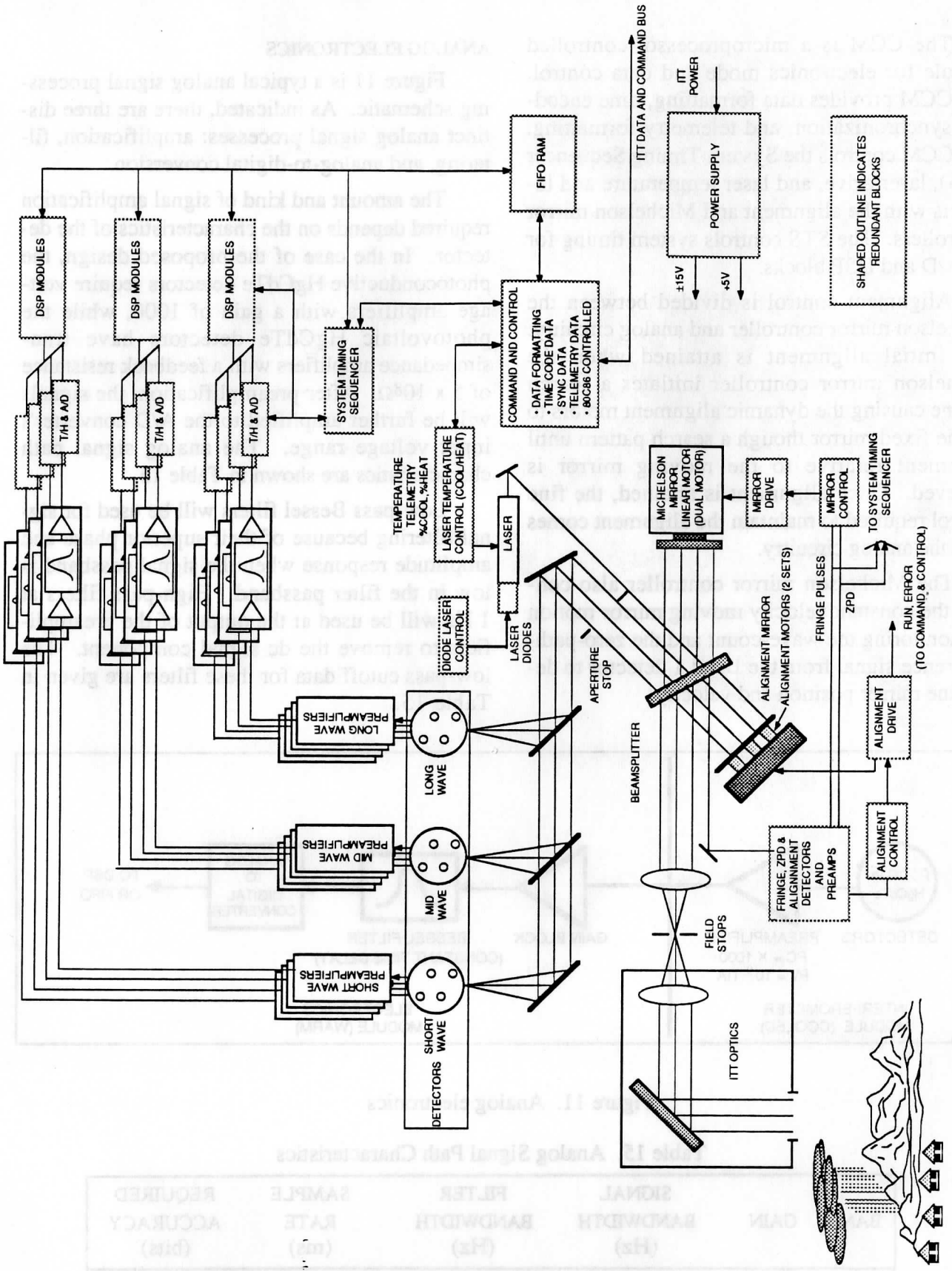

Figure 10. Electronics block diagram for the point design

The CCM is a microprocessor-controlled module for electronics mode and data control. The CCM provides data formatting, time encoding, synchronization, and telemetry formatting. The CCM controls the System Timing Sequencer (STS), laser drive, and laser temperature and interacts with the alignment and Michelson mirror controllers. The STS controls system timing for the A/D and DSP blocks.

Alignment control is divided between the Michelson mirror controller and analog circuitry. The initial alignment is attained when the Michelson mirror controller initiates a search routine causing the dynamic alignment motors to tilt the fixed mirror though a search pattern until alignment relative to the moving mirror is achieved. Once alignment is attained, the fine control required to maintain the alignment comes from the analog circuitry.

The Michelson mirror controller also controls the constant velocity moving mirror motion by monitoring the wave-count and the zero-path-difference signal from the Band 1 detector to determine mirror position and velocity.

ANALOG ELECTRONICS

Figure 11 is a typical analog signal processing schematic. As indicated, there are three distinct analog signal processes: amplification, filtering, and analog-to-digital conversion.

The amount and kind of signal amplification required depends on the characteristics of the detector. In the case of the proposed design, the photoconductive HgCdTe detectors require voltage amplifiers with a gain of 1000, while the photovoltaic HgCdTe detectors have transimpedance amplifiers with a feedback resistance of $5 \times 10^8 \Omega$. After preamplification, the signals will be further amplified to the A/D converter's input voltage range. The analog signal path characteristics are shown in Table 15.

Low-pass Bessel filters will be used for signal filtering because of their superior phase and amplitude response when the signal passband is low in the filter passband. High-pass filters at 1 Hz will be used at the output of the preamplifiers to remove the dc signal component. The low-pass cutoff data for these filters are given in Table 15.

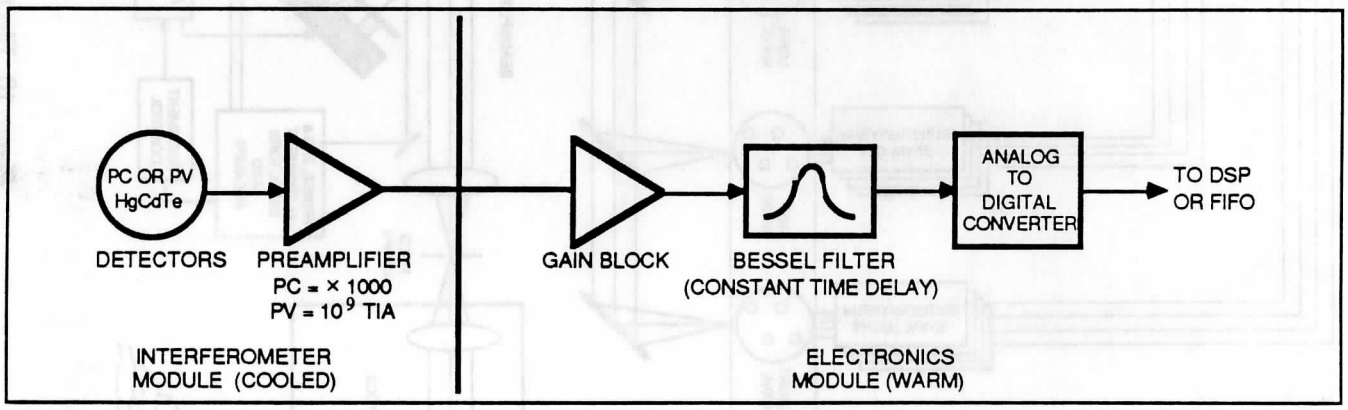

Figure 11. Analog electronics

Table 15. Analog Signal Path Characteristics

BAND	GAIN	SIGNAL BANDWIDTH (Hz)	FILTER BANDWIDTH (Hz)	SAMPLE RATE (ms)	REQUIRED ACCURACY (bits)
1	7700	2480-4600	1-9434	53.0	14
2	25000	4840-6960	1-18868	26.5	13
3	33.3	8600-10240	1-18868	26.5	12

DIGITAL SIGNAL PROCESSING

The digitized interferograms from the four detectors of one band are stored in parallel in the memory buffer of a single Digital Signal Processor (DSP) module, as indicated in Figure 12. The DSP module integrated circuit is a Texas Instruments SMJ320C25 (military version of the TMS320C25); a very fast dedicated processor. The TMS320 applies a digital filter to the raw interferogram to reduce the number of points and subsequently performs a radix 4 Fast Fourier Transform (FFT) to compute the raw spectra. The detailed filter and FFT parameters, including relevant timing information, are shown for all three resolution modes in Table 16. This process is performed in parallel for the three spectral bands.

TMS320 Family Digital Signal Processors

The TMS320C25 is a digital signal processor that is well suited for use in space applications. It is:

- Capable of performing 10-million instructions per second.
- Uses only 725 mW (average) power at the highest clock rate.
- Fabricated using CMOS technology so power consumption is clock-rate dependent.
- Manufactured by Texas Instruments, a well-recognized name in the electronics industry, ensuring continued part availability and support.

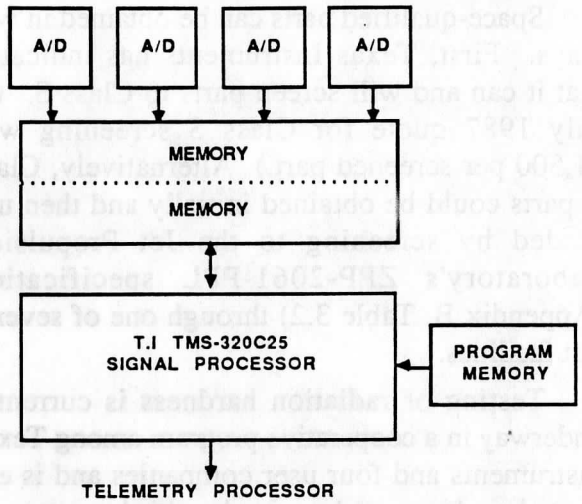

Figure 12. Digital signal processor module design

Table 16. On Board Processing Parameters

Mode	Band	Laser Sample Skip Factor	# Input Pts/FOV	Digital Filter/FOV		FFT(Radix 4) Time(ms)/FOV	# In band Pts/FOV	Total* Time(sec)
				Time(ms)	# Pts Out			
High Resolution	1	2	14623	19	4K complex	69	3680	0.352
	2	1	8189	10	1K complex	28	920	0.152
	3	1	8189	10	1K complex	28	991	0.152
Medium Resolution	1	2	7076	10	4K real	40	1841	0.200
	2	1	8189	10	1K complex	28	920	0.152
	3	1	8189	10	1K complex	28	991	0.152
Low Resolution	1	2	1416	5	1K complex	14	460	0.076
	2	1	2038	5	1K complex	14	230	0.076
	3	1	2038	5	1K complex	14	248	0.076

* Total time/dwell = (4 FOV/band)x(Digital filter time/FOV+FFT time/FOV), because a single DSP performs the processing for each band. Total times must be less than 0.8, 0.4, 0.1 seconds for High, Medium, and Low Resolution modes.

The power requirements for on-board processing are relatively small because of the use of CMOS memories, which require very little power when not being accessed.

The TMS320C25 has been commercially available since June 1987, and breadboard parts have been received by SBRC for use on the Thermal Emission Spectrometer instrument for the Mars Observer Mission. The military-qualified part is designated SMJ320C25 and has been available since November 1987. The SMJ prefix indicates routine part screening to MIL-STD-883, Rev. C, Class B.

Space-qualified parts can be obtained in two ways. First, Texas Instruments has indicated that it can and will screen parts to Class S. (A July 1987 quote for Class S screening was $1,500 per screened part.) Alternatively, Class B parts could be obtained initially and then upgraded by screening to the Jet Propulsion Laboratory's ZPP-2061-PPL specification (Appendix B, Table 3.2) through one of several test facilities.

Testing of radiation hardness is currently underway in a cooperative program among Texas Instruments and four user companies and is expected to be complete in the third quarter of 1988. Test data on other, similar, Texas Instrument parts indicate that radiation hardness should not be a problem. For instance, test data on the TMS27C256, a 256-kbit UV EPROM, shows a radiation hardness of 13 krad (Si), total dose to specification; 20 to 25 krad (Si), total does functionality; and 1.67 to 1.88 $\times 10^{10}$ rad (Si)/second, dose rate with no single-event upsets and no latchup. Both parts are fabricated using similar processes.

Destructive part analysis per MIL-STD-883C, Method 5009, is currently underway at SBRC for the Mars Observer Mission.

DSP Module Power Budget

The DSP power budget is presented in Table 17. Note that the individual memories will be in a non-power-consuming mode for approximately 90% of the time.

CONTROL SYSTEMS

The following electronics control systems are required; an overall command and control system, a system timing sequencer to control data flow from the analog-to-digital converters, a Michelson mirror controller to synchronize moving mirror scans with the pointing mirror, and an alignment controller for the dynamic alignment system.

Table 17. DSP Power Budget

Processor	
TMS320C25 @ 10 MHz	504 mW
Active Memories	
Active Program Bank	414 mW
Processor Side Data Bank	120 mW
A/D Side Data Banks (4)	690 mW
	1.739W
Total Power for 3 Modules	5.2W

Command and Control

The Command and Control Module (CCM) is responsible for overall spectral resolution control. Associated tasks include, interface to the spacecraft, alignment and Michelson-mirror controllers, laser drive control, laser system temperature control, system timing sequencer spectral resolution control, and first-in first-out (FIFO) memory control, as well as telemetry formatting, synchronization, and time encoding. This module consists primarily of an HS 80C86 microprocessor system. Associated drive circuit functions are subsets of other functional blocks. The CCM will control the output of the laser diodes. The FIFO memory buffers the data onto the spacecraft bus. There is no stated requirement for this memory, however, the data rate without it would be nonuniform. This memory is implemented as RAM under control of the Command and Control Module (CCM). The CCM receives periodic data requests, addresses the RAM, and signals the spacecraft that bus data are valid, whereupon the spacecraft reads the data. The CCM has two pointers: the next address to load new data into and the next address to output to the spacecraft. When new data are loaded into RAM, the first pointer is incremented; when data are output onto the data bus, the second pointer is incremented. When the end of the RAM is addressed, the pointer is reset to the beginning of the RAM. The overall effect is the RAM acts as a revolving queue that looks like a FIFO memory.

System Timing Sequencer

The system timing sequencer controls the overall data flow from the A/D converters to the DSP modules and into the FIFO memory. The A/D converters begin the conversion process a fixed time after the sample pulse, allowing the electrical signal to propagate through the electrical filters equally. This delay time is slightly different for each band and for each detector, and the appropriate delay time is established here. Data are then read into the DSP modules, and the output data are read into the FIFO in a specified sequence. All the handshaking among these modules is contained in this block. Since the sequence is constant and cyclic, the block can be implemented with counters and Programmable Read Only Memory (PROM).

Michelson Mirror Control

The microprocessor-driven Michelson mirror controller has two basic functions. First, it contains the logic necessary to send the dynamic alignment mirror through a search pattern to acquire optical alignment and then to transfer the maintenance of that alignment to special analog circuitry. Secondly, the Michelson mirror controls the moving mirror velocity and extent of travel corresponding to the low, medium, and high resolution modes defined in Table 3 for Band 1.

Alignment Control

Alignment control will be implemented using two control loops. At start up, the Michelson mirror controller will take control from the local analog control loop and perform a search pattern to align the optical system. When alignment has been attained, alignment control will be returned to the analog control system. The analog control system only needs to maintain alignment. The alignment control system is a simple x-y control system using orthogonal alignment fringes and fringe detectors.

POWER

The breakdown of power requirements for the interferometer assembly and the net increase in power required for the interferometer are given in Table 18.

Table 18. Power Consumption Breakdown for the Interferometer Assembly

SUBSYSTEM	POWER (W)
Digital Signal Processors	5.2
Command and Control Module	3.0
Michelson Mirror Drive	8.5
Dynamic Alignment Mirror Drive	3.2
Laser	1.0
	20.9
Total Power for ITT Filter Wheel	10.2
Net Power Increase	10.7

PARTS NOT ON THE APPROVED PARTS LIST

Table 19 lists parts expected to be in the proposed sounder design, but not on the "Program Approved Parts List For GOES Imager and Sounder (Rev. H)," prepared by ITT Aerospace/Optical Division. The list is important when considering the long lead time required to procure parts for space sensor applications.

Table 19. Parts Not on the GOES Rev H Approved Parts List

PART NUMBER	DESCRIPTION	VENDOR	COMMENT*
SMJ320C25[1]	Digital Signal Processor	Texas Instruments	1
HC6264R	Random Access Memory	Honeywell	1, 2
HS6617	Programmable. Read Only Memory	Harris	3
HS9476	A/D converter	Hybrid Systems	4
LT1028	Operational Amplifier	Linear Technology	5
TBD	Laser Diode	Spectra Diode Labs	6
MSR-3	Resistor	Mini Systems Inc.	7
HC-80C86RH	Microprocessor	Harris	8
HC-82C85RH	Clock Generator	Harris	9

*Notes:

1. This part is critical to the digital signal processor module.
2. This RAM is 16 times more dense than the approved parts list RAM.
3. This PROM is required for its very low OFF current.
4. The approved A/D converter is only accurate to 9 bits, 14 bit accuracy is required.
5. This operational amplifier is required to maintain the signal to noise ratio.
6. The laser diode is required for laser fringe generation.
7. Required for high bandwidth and low noise in preamplifier.
8. SBRC has verbal instructions from ITT indicating this part will be available for this mission.
9. This part is a companion to the HC-80C86RH and is required for clock generation.

[1]The SMJ320C25 is the military version of the TMS320C25.

Section 4
MECHANICS

MECHANICAL DESIGN GOALS

The mechanical design goals were to:

- Replace the GOES L,M filter wheels with an interferometer.
- Design a replacement package that will fit within the existing aft optics/filter-wheel space.
- Design the interferometer to be a modular, bolt-on unit weighing approximately the same as the displaced subassembly, i.e., about 10 pounds.
- Preserve the alignment of the units to the existing ITT radiative coolers.
- Design all moving elements to a 5-year lifetime.

Detailed ITT drawings of the GOES I/M Sounder baseplate, vacuum housing, primary mirror mount, and optical elements were used to create an interface model as the baseline. Several interferometer optical elements were added to the baseline model, and Figure 13 represents the current optomechanical design.

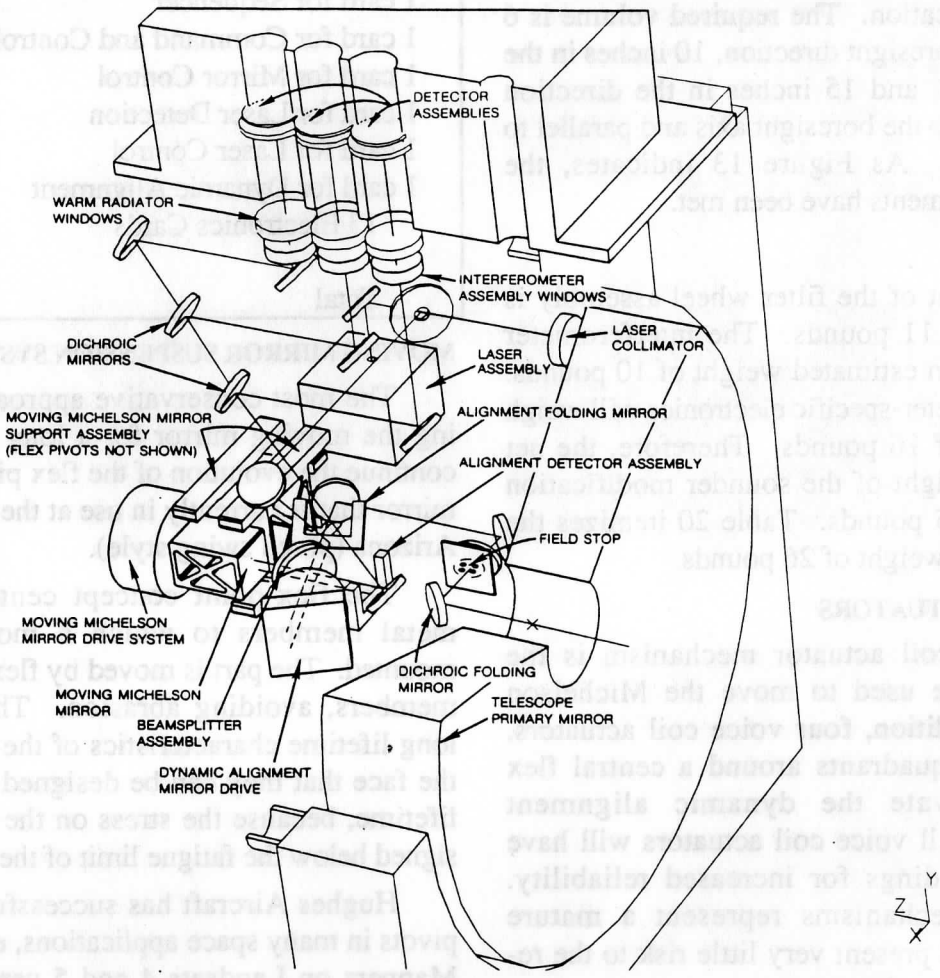

Figure 13. Optomechanical design

As shown in Figure 13, the laser will be mounted on the baseplate; the optics required to relay the laser beam to the interferometer assembly will be packaged as part of the laser subassembly. The Michelson moving mirror, dynamic alignment mechanism, and associated optical elements will be mounted in a common structure. The fixed end of the moving mirror mechanism and the mechanical ground of the voice coil actuator will be mounted on the subassembly structure. The fixed end of the dynamic alignment mechanism must be fastened to the same mechanical ground as the fixed end of the moving mirror.

VOLUME

Packaging for the optical systems was optimized through careful analysis and design. Extensive modeling on GEOMOD resulted in a package that will fit well into the existing GOES filter-wheel location. The required volume is 6 inches in the boresight direction, 10 inches in the nadir direction, and 15 inches in the direction perpendicular to the boresight axis and parallel to the baseplate. As Figure 13 indicates, the volume requirements have been met.

WEIGHT

The weight of the filter wheel assembly is approximately 11 pounds. The interferometer assembly has an estimated weight of 10 pounds. The interferometer-specific electronics will weigh on the order of 16 pounds. Therefore, the net increase in weight of the sounder modification will be only 15 pounds. Table 20 itemizes the estimated total weight of 26 pounds.

VOICE COIL ACTUATORS

A voice coil actuator mechanism is the primary device used to move the Michelson mirror. In addition, four voice coil actuators, positioned in quadrants around a central flex column, activate the dynamic alignment mechanism. All voice coil actuators will have redundant windings for increased reliability. Voice coil mechanisms represent a mature technology and present very little risk to the reliability of the interferometer.

Table 20. Estimated Weight of the Interferometer and Electronics Subassembly

COMPONENT	ESTIMATED WEIGHT (lbs)
Outer Structure	3.0
Registration Mounts	2.0
Optical Elements	0.6
Optical Holders	1.0
Laser and Mount	0.4
Moving Mirror Subsystem	0.5
Dynamic Motion alignment mechanism	0.4
Cold "Strapping"	1.0
Cables/Fasteners	1.0
Subtotal Mechanical	10.0
6 cards for DSP Modules	7.6
1 card for FIFO and Power Supply	1.2
1 card for Sequencer	1.2
1 card for Command and Control	1.2
1 card for Mirror Control	1.2
1 card for Laser Detection	1.2
1 card for Laser Control	1.2
1 card for Dynamic Alignment	1.2
13 Electronics Cards	16.0
Total	26.0

MOVING MIRROR SUSPENSION SYSTEM

The most conservative approach to designing the moving mirror for a long lifetime is to continue the evolution of the flex pivot supported mirror that is currently in use at the University of Arizona (porch swing style).

The flex-point concept centers on using metal members to which a moving part is mounted. The part is moved by flexing the metal members, avoiding abrasion. The key to the long lifetime characteristics of the flex points is the face that they can be designed for "infinite" lifetime, because the stress on the fixture is designed below the fatigue limit of the material.

Hughes Aircraft has successfully used flex pivots in many space applications, e.g., Thematic Mappers on Landsats 4 and 5 use them on the scan mirror, scan line corrector, redundant shutter, and main calibration/restore shutter. One

of SBRC's first cloud cameras used flex pivots that operated for 10 years; the Hughes VM cryogenic cooler uses three flex pivots and recently passed 32,000 hours of operation at 300 RPM without a pivot failure.

However, special screen testing is necessary in order to qualify each of these commercial Bendix pivots and the yield has not been impressive. In addition, the difficulty of selecting pivots with compatible center shifts and spring rates for the moving mirror is considerable. Therefore, SBRC has funded IR&D tasks in the generic area of "Scan Drive Mechanisms" for several years. One of the key tasks has been to develop structural pivots that are space-flight quality, exhibit a minimum center shift during angular rotation, have more predictable spring rates, and have an improved processing yield. Two such pivot designs have been completed--the Torsion Pivot and the Bi-Flex Pivot. Five units of each design were fabricated and assembled. Each unit has successfully completed spring rate measurement, hysterisis checks, center shift under 10 degree rotation, and a run-in cycle test of 5.5 million cycles. All 10 units have been found acceptable, based on existing Enhanced Thematic Mapper specifications. Both design types show center shifts much lower than commercial pivots.

Figure 14 shows the porch-swing type of flex pivot for the moving mirror that uses six structural pivots with minimal center shift and matched spring rates. Further tooling development and design refinements tailored to the GOES application are required, but the approach can meet the challenge of making a compact, large-deflection, long-lifetime moving mirror.

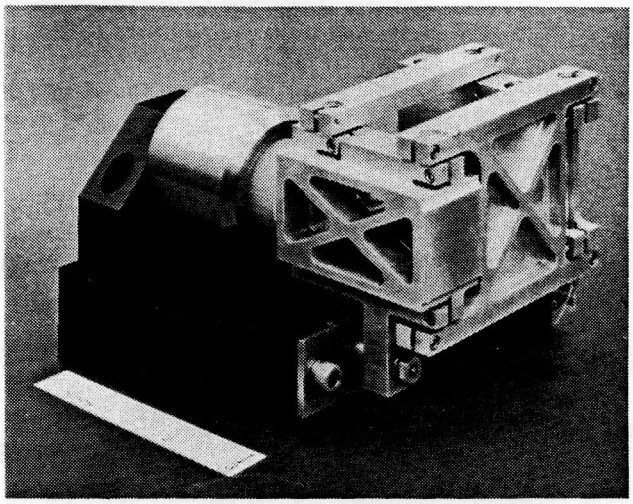

Figure 14. Optical path difference mirror drive actuator for HIS GEO application

An alternate moving-mirror flex-pivot design concept has recently been proposed for project AIRS. Figure 15 shows flexure elements arranged to constrain a moving mirror to follow a straight line. Design tradeoffs have been performed under SBRC IR&D funding, and detailed drawings of the piece parts and assembly have been completed. The design particulars do not fit the GOES requirement exactly, but the concept is suitable for the endurance limit operation necessary for the 5-year lifetime. Further evaluation of this design is anticipated.

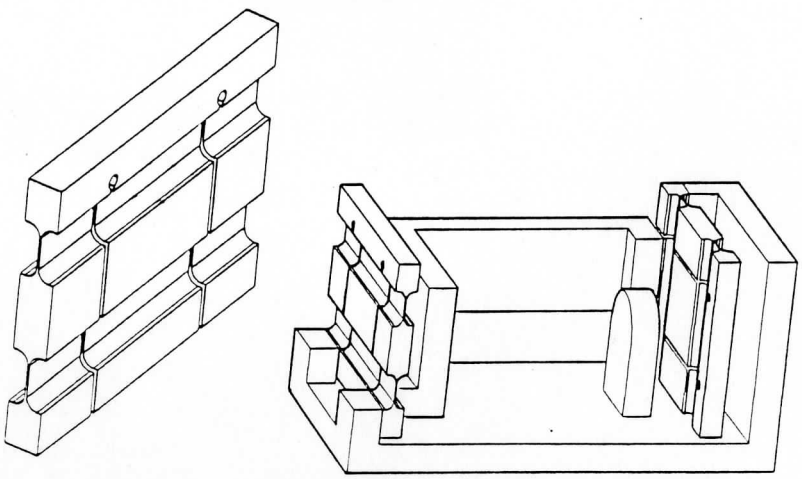

Figure 15. Alternate flex pivot design for the Michelson mirror mechanism

APPENDIX A

VARIABLE VELOCITY MICHELSON MOVING MIRROR

(UNIVERSITY OF WISCONSIN)

Appendix A
VARIABLE VELOCITY MICHELSON MOVING MIRROR

SUMMARY OF HIS INSTRUMENT TESTS

The value of a variable velocity Michelson moving mirror lies in the fact that it permits the information contained within an interferogram to be "optimally" scanned. For example, the interferogram corresponding to the 15 μm CO_2 sounding region has a resonance centered at approximately 0.7 cm optical delay that contains much of the information about CO_2 line structure. For the purpose of temperature sounding with CO_2, it would be useful to be able to move the OPD scan mirror quickly out to the resonance region and then to scan through the resonance more slowly, thereby improving the signal-to-noise ratio for the high-spectral-resolution information.

A test of the feasibility of the variable velocity scanning approach was designed and implemented at the UW-SSEC using the HIS aircraft instrument. A specially designed and built scan-mirror velocity controller was used to drive the Michelson mirror through its ± 2 cm OPD travel at a speed that was completely programmable under microprocessor control. Figure A-1 shows the input speed profile, v(t), to which the moving mirror was driven. The shape of this profile shows that the moving mirror begins its scan at -X, passing through the resonance at -0.7 cm at a slow scan rate, rapidly accelerates, then scans through the ZPD region at a higher (four times) constant rate of speed, decelerates, and continues to scan to +X at the slower scan rate.

To test the feasibility of the variable velocity scan method, data was taken with the instrument in both the (normal) constant velocity mode and in the variable scan mode during a period of constant scene conditions. Data taken in these two modes was later analyzed and compared in order to identify artifacts that may have been introduced by the variable velocity scan.

In order to run the test for a true atmospheric spectrum, the downwelling radiation of the sky was observed from the roof of the Space Sciences building in Madison with the HIS scene mirror pointing towards zenith. Examples of the downwelling spectra for HIS Band 1, comparing constant and variable-scan spectra under nearly constant viewing conditions, are shown in Figure A-2. The atmospheric CO_2, H_2O and O_3 absorption line structure is readily apparent in this figure. This comparison shows that, within the uncertainty due to atmospheric variability (a few tenths of a degree), the variable-velocity scan mode does not introduce artifacts in the spectra when proper attention is paid to the interferometer sampling system.

The major sampling-system requirement is that the time delay associated with the analog filtering of the IR interferogram (for noise minimization) must be matched by delaying the laser sample trigger. This prevents optical-path-difference sampling errors (Michelson mirror position errors) proportional to the velocity variations and to the time delay mismatch. A discussion of the electrical design issues important to proper interferogram sampling is given in the next subsection.

Because the HIS sky-viewing demonstration of the variable velocity Michelson mirror is limited to an accuracy of a fraction of a degree by the size of true atmospheric variations, it is useful to understand the potential error mechanism theoretically. This will make it possible to predict the size of any residual errors. For the velocity profile of Figure A-1 and the interferogram of the 15 μm CO_2 band of interest here, optical-path-difference sampling errors, δx, from velocity variations translate into phase errors, $\delta\phi$, of the high-resolution contribution to the spectrum (mainly from delays greater than 0.5 cm scanned at an OPD velocity of v_h=0.15 cm/s) relative to the low-resolution spectrum (from delays less than 0.25 cm scanned at v_l=0.6 cm/s). The phase error is given by:

$$\delta\phi = 2\pi\nu\,\delta x = 2\pi\nu\,(v_l\tau_l - v_h\tau_h) \quad (1)$$

where ν is the wavenumber and τ_l and τ_h are the low- and high-resolution sampling system time delay mismatches. For an analog design in which the time delay mismatch depends on

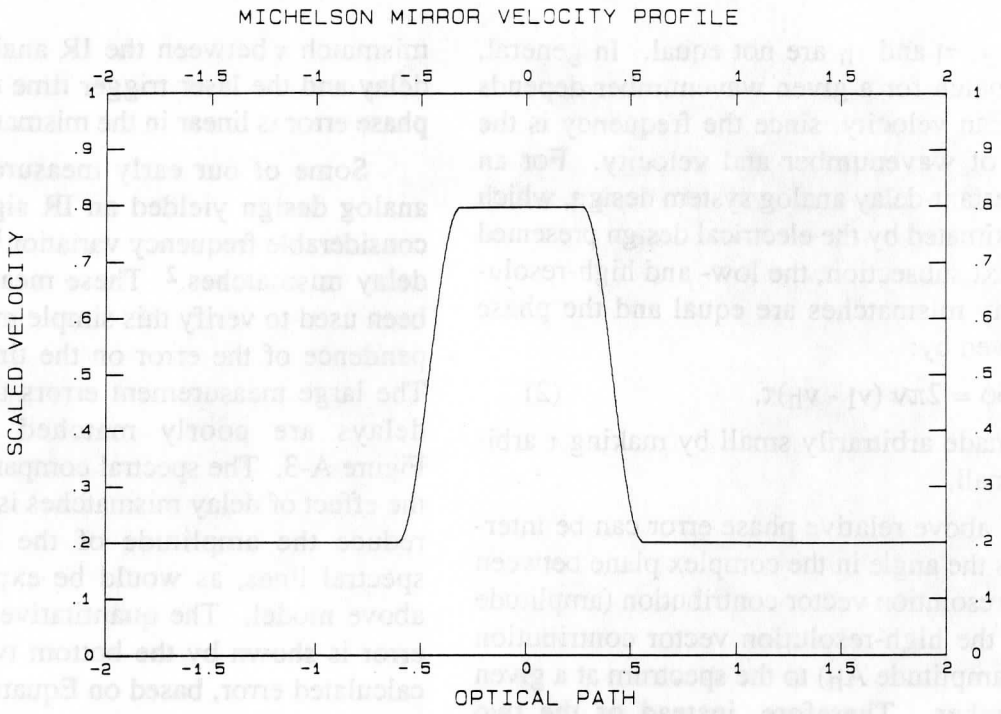

Figure A-1. The Michelson mirror velocity profile used to make a variable velocity OPD scan. The actual mirror OPD velocities were 0.6 cm/sec near ZPD and 0.15 cm/sec in the region of large delay.

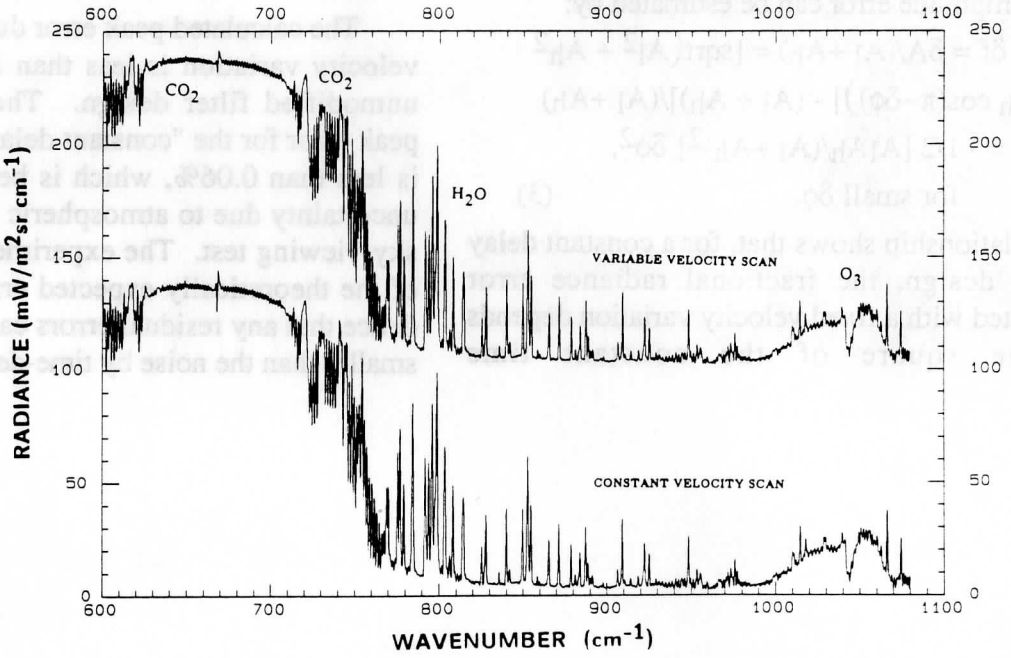

Figure A-2. A comparison of nearly coincident observations (June 9, 1988) of downwelling radiance spectra using both a constant mirror velocity and the variable velocity profile of Figure A-1. The excellent agreement shown is made possible by a careful adjustment of the analog filter delay dependence in order to make the interferogram sampling frequency independent. (See Figure A-7.)

frequency, τ_l and τ_h are not equal. In general, the mismatch for a given wavenumber depends on the scan velocity, since the frequency is the product of wavenumber and velocity. For an ideal constant-delay analog system design, which is approximated by the electrical design presented in the next subsection, the low- and high-resolution delay mismatches are equal and the phase error, given by:

$$\delta\phi = 2\pi\nu\,(v_l - v_h)\tau, \qquad (2)$$

can be made arbitrarily small by making τ arbitrarily small.

The above relative phase error can be interpreted as the angle in the complex plane between the low-resolution vector contribution (amplitude A_l) and the high-resolution vector contribution (signed amplitude A_h) to the spectrum at a given wavenumber. Therefore, instead of the two contributions adding as scalars, which they would if the relative phase error were zero, they add as non-colinear vectors. The resulting fractional amplitude error can be estimated by:

$$\delta f = \delta A/(A_l + A_h) = [\mathrm{sqrt}(A_l^2 + A_h^2 - 2A_lA_h\cos(\pi - \delta\phi))] - (A_l + A_h)]/(A_l + A_h)$$
$$= -1/2\,[A_lA_h/(A_l + A_h)^2]\,\delta\phi^2, \quad \text{for small } \delta\phi. \qquad (3)$$

This relationship shows that, for a constant delay analog design, the fractional radiance error associated with a fixed velocity variation depends on the square of the constant time mismatch τ between the IR analog signal time delay and the laser trigger time delay, since the phase error is linear in the mismatch.

Some of our early measurements with an analog design yielded an IR signal delay with considerable frequency variation[1] and large time delay mismatches.[2] These measurements have been used to verify this simple model for the dependence of the error on the timing mismatch. The large measurement errors that result when delays are poorly matched are shown in Figure A-3. The spectral comparisons show that the effect of delay mismatches is to substantially reduce the amplitude of the high-resolution spectral lines, as would be expected from the above model. The quantitative analysis of the error is shown by the bottom two curves. The calculated error, based on Equation 3, shows the same spectral character as the measured error, but differs by about a factor of two in amplitude. This level of agreement is very good considering the simplicity of the model used in the analysis.

The calculated peak error due to the imposed velocity variation is less than about 6% in the unmodified filter design. The corresponding peak error for the "constant delay" analog design is less than 0.06%, which is below the level of uncertainty due to atmospheric variations in the sky-viewing test. The experimental verification of the theoretically expected errors gives confidence that any residual errors can easily be made smaller than the noise by time-delay matching.

[1] 1738 to 78 ms compared to 48 to 13 ms for the "constant delay" design (62 ms laser trigger delay).

[2] 1738 to 78 μs compared to 48 to 13 μs for the "constant delay" design (62 μs laser trigger delay).

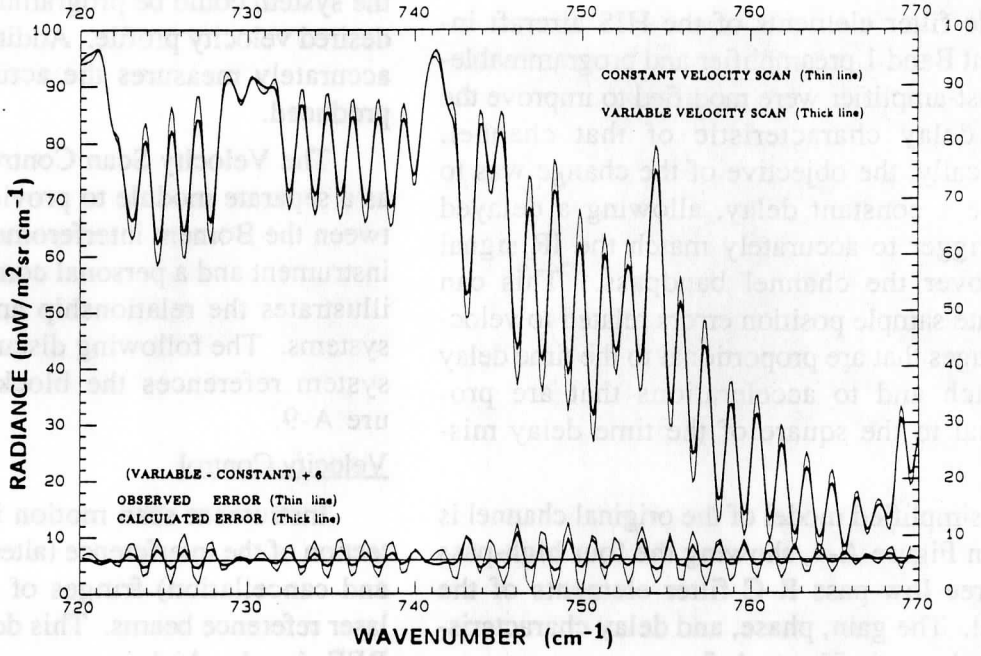

Figure A-3. A comparison of downwelling radiance spectra observed (January 15, 1988) under uniform sky viewing conditions showing the error introduced when the interferogram sampling in delay is not frequency independent. (See Figure A-5.)

AMPLIFIER/ANALOG-FILTER MODIFICATION

The filter elements of the HIS aircraft instrument Band 1 preamplifier and programmable-gain post-amplifier were modified to improve the group delay characteristic of that channel. Specifically, the objective of the change was to produce a constant delay, allowing a delayed laser trigger to accurately match the IR signal delay over the channel bandpass. This can eliminate sample position errors related to velocity changes that are proportional to the time delay mismatch and to accelerations that are proportional to the square of the time delay mismatch.

A simplified model of the original channel is given in Figure A-4, showing the four high-pass and three low-pass R-C filter elements of the channel. The gain, phase, and delay characteristics are shown in Figure A-5.

The channel was modified to eliminate all high-pass filter elements except for the coupling network at the output of the first stage, needed to block the dc offset generated by the detector bias supply (not shown in the model). The original post-amplifier circuit was replaced by a single dc-gain stage followed by a four-pole, low-pass, constant-delay filter with a nominal cutoff frequency of 7 kHz. A model of the Band 1 channel after modification and the resulting characteristics are shown in Figures A-6 and A-7, respectively.

In the frequency range of 255 Hz to 735 Hz, the variation in group delay for the unmodified and modified channels are 279.8 μs and 4.6 μs, respectively. The residual delay variation in this frequency range for the modified channel is almost entirely due to the high-pass coupling network between the first two stages and can be reduced, if desired, to an arbitrarily small value by changing component values or other redesign.

VARIABLE VELOCITY CONTROLLER SYSTEM

To support investigations on the benefits of using various speeds in the course of an interferometer scan, a Velocity Scan Controller System (VSCS) was constructed to permit control of the HIS Aircraft Instrument (HIS/AE) scan velocity in a completely general way; i.e., the system could be programmed to produce any desired velocity profile. Additionally, the system accurately measures the actual scan velocities produced.

The Velocity Scan Controller was designed as a separate module to provide an interface between the Bomem interferometer within the HIS instrument and a personal computer. Figure A-8 illustrates the relationship among the different systems. The following discussion of the VSCS system references the block diagram of Figure A-9.

Velocity Control

Instrument scan motion is indicated by detection of the interference (alternate reinforcement and cancellation) fringes of the interferometer laser reference beams. This detector output is the REF signal, which serves as the basis for all instrument data sampling timing. The laser wavelength is such that 15,799 REF pulses are generated for each centimeter of mirror travel. Another HIS/AE signal, MSB, is a bilevel signal that indicates the direction of the scan in progress.

The REF signal, divided by two, is used to increment a Sample Counter in the VSCS. The content of this counter, which is reset with each change in direction, along with the MSB signal, provides the VSCS with both scan position and scan direction information. The Sample Counter output and the MSB signal form the address input to a random access memory (RAM), which contains the data representing the desired velocity profile. Note that since the MSB signal is one of the RAM address bits, it is possible to program a different velocity profile for each of the two scan directions. The RAM size permits velocity control for scan lengths of up to the instrument maximum of 3.6 cm with a value assignment for every two instrument samples.

In the normal aircraft instrument system, the scan motor speed is proportional to the voltage of a control signal labelled DIR. Normally, a tachometer feedback control loop, termed "speed trim," adjusts the DIR voltage as necessary to maintain the desired speed within ±10%. When

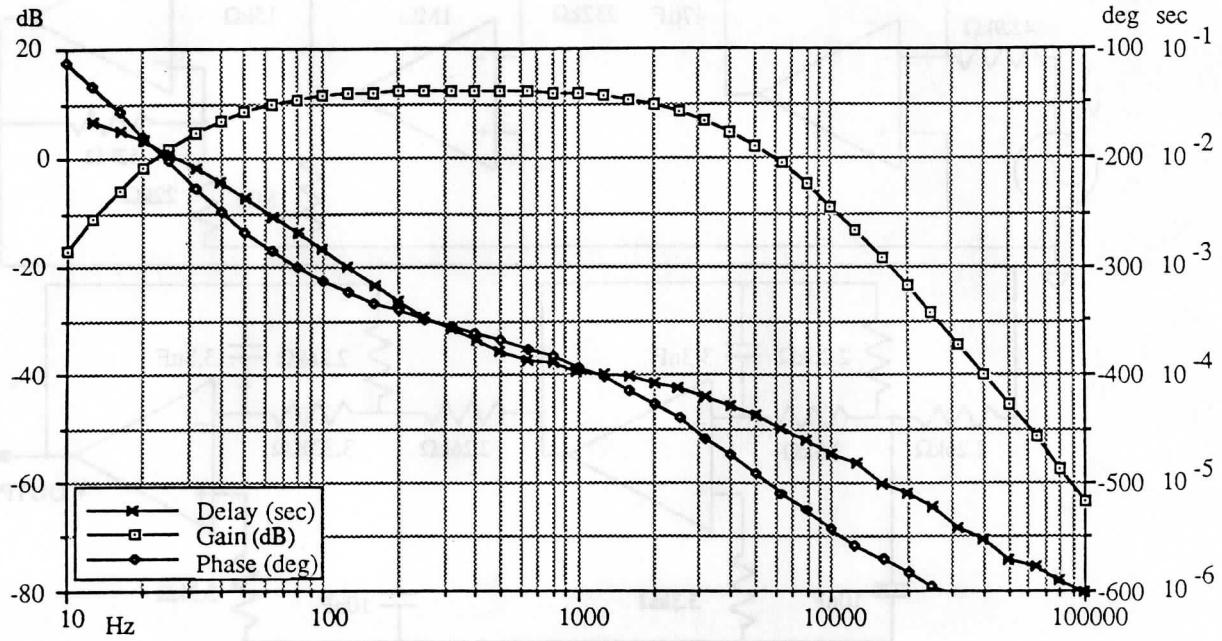

Figure A-4. HIS Band 1 original amplifier schematic

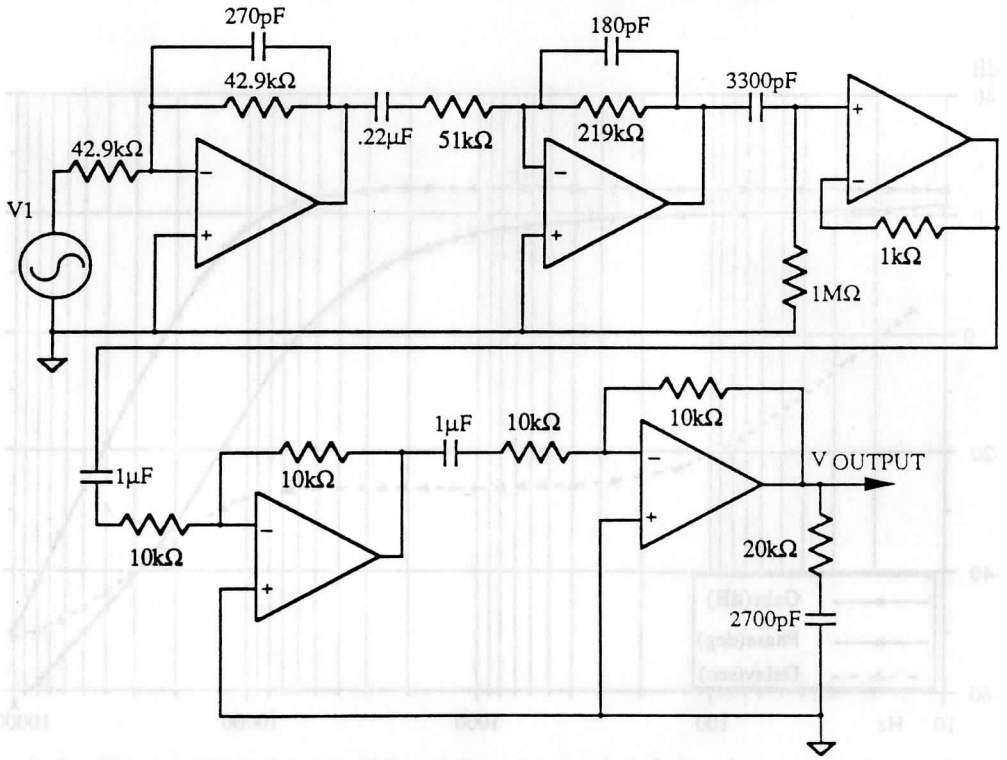

Figure A-5. Original Band 1 amplifier gain, phase, and delay frequency dependence

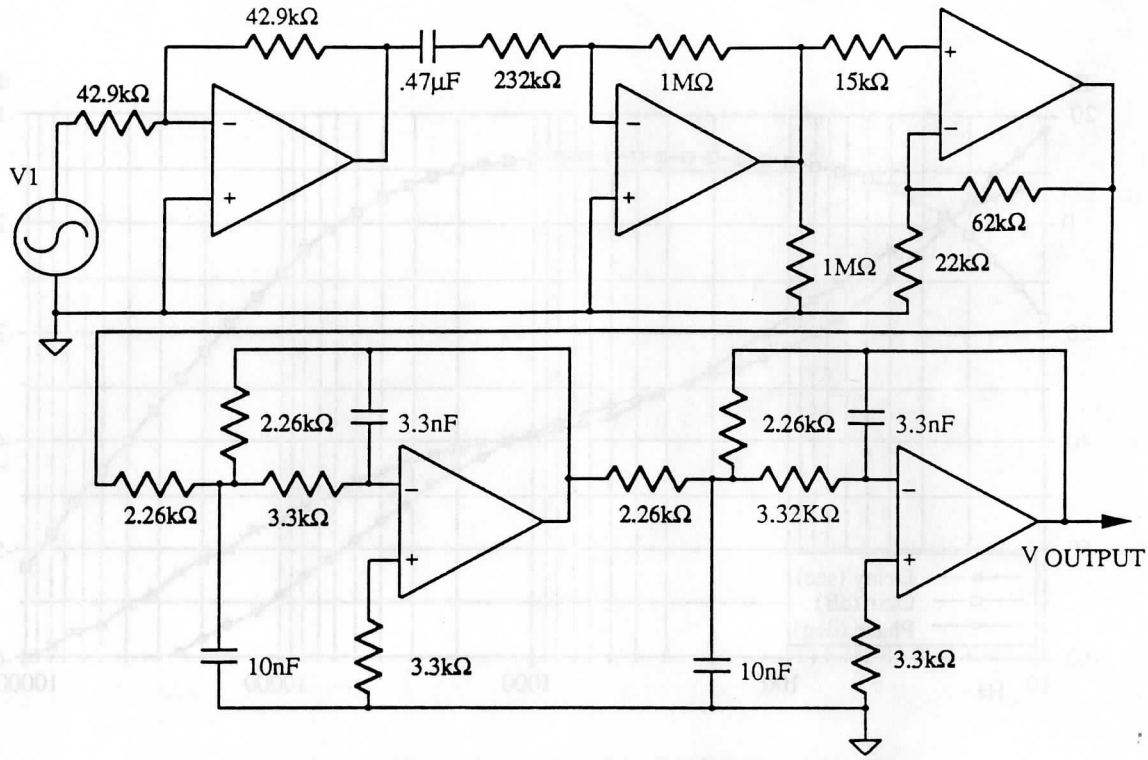

Figure A-6. HIS Band 1 modified amplifier schematic

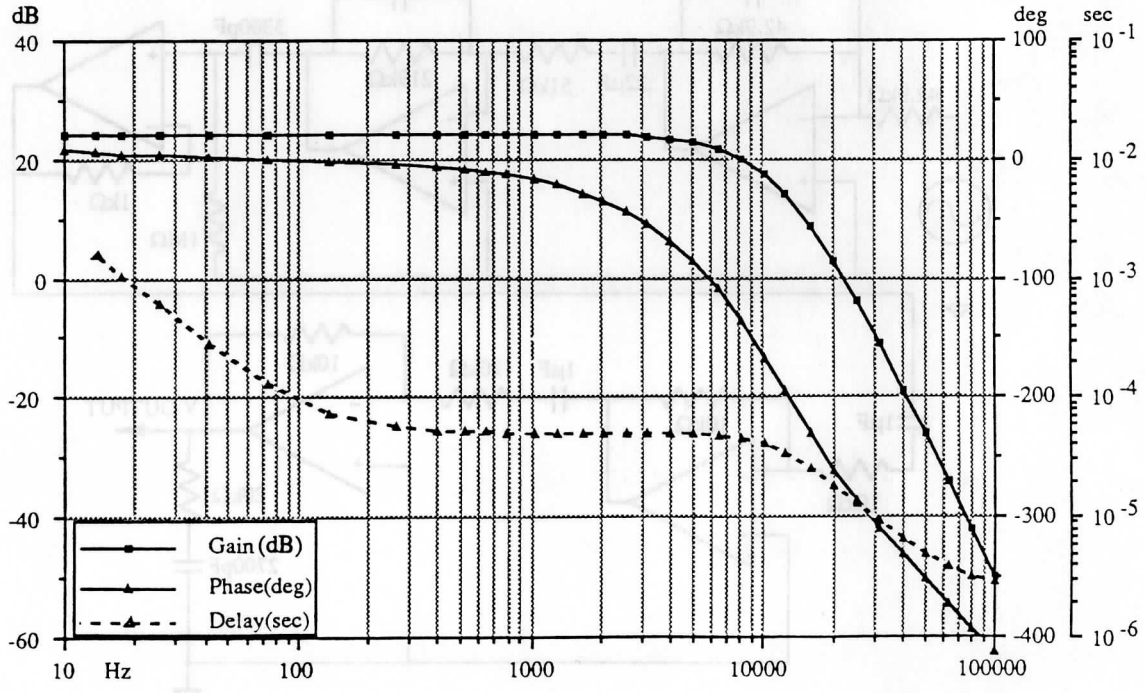

Figure A-7. Modified Band 1 amplifier gain, phase, and delay showing the frequency independence of the delay

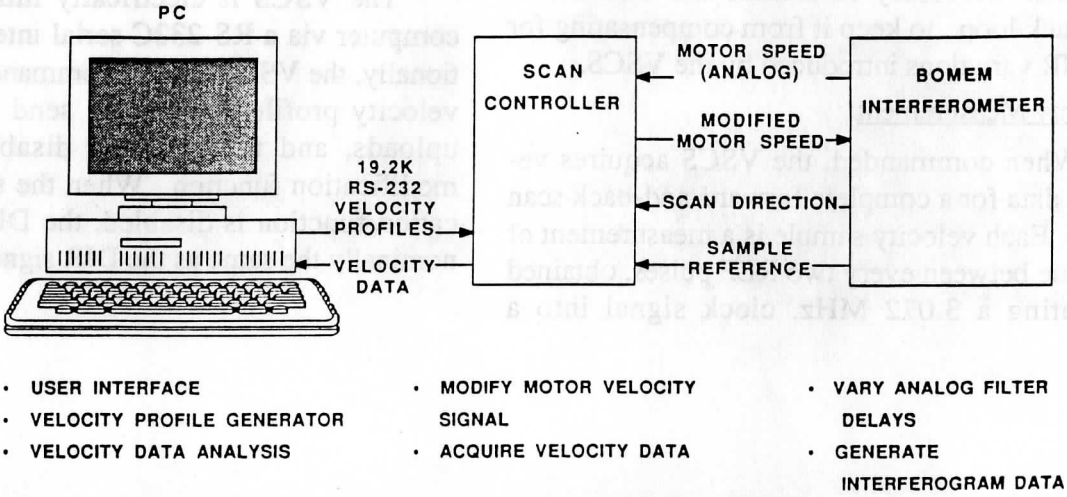

Figure A-8. Variable scan speed system

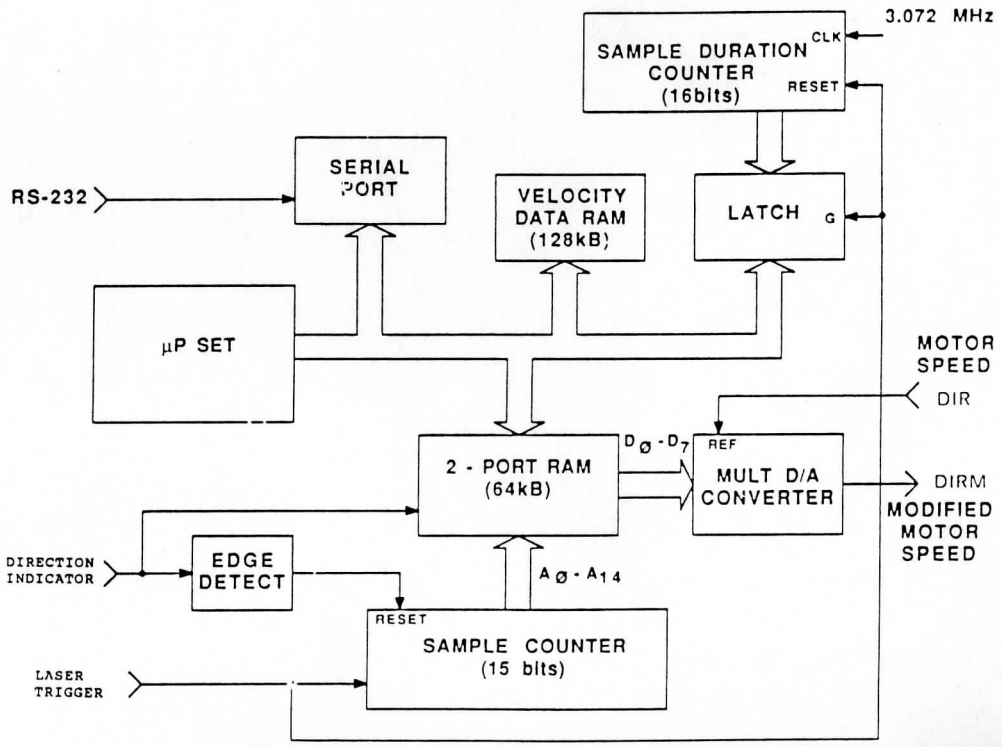

Figure A-9. Scan controller block diagram

the VSCS is employed, the DIR input to the motor drive amplifiers is replaced by a DIRM control signal. The magnitude of the DIRM signal is a fraction of that of the DIR, the fraction determined by the value programmed into the RAM. It is also necessary to disable the tachometer feedback loop , to keep it from compensating for the DIR variations introduced by the VSCS.

Velocity Measurement

When commanded, the VSCS acquires velocity data for a complete forward-and-back scan cycle. Each velocity sample is a measurement of the time between every two REF pulses, obtained by gating a 3.072 MHz. clock signal into a counter for the sample duration. Samples are transferred to a Velocity Data RAM with sufficient capacity to store the data from a complete scan cycle.

System Control

The VSCS is electrically linked to a host computer via a RS-232C serial interface. Functionally, the VSCS may be commanded to receive velocity profile downloads, send velocity data uploads, and to enable or disable the speed modification function. When the speed modification function is disabled, the DIRM signal is nominally the same as the DIR signal.